

3-31-2023

RECOMBINANT DNA VACCINE DESIGN AS A POTENTIAL STRATEGY AGAINST BOVINE FOOT AND MOUTH DISEASE VIRUS (FMDV)

Taylor Haynie

Louisiana State University and Agricultural and Mechanical College

Follow this and additional works at: https://digitalcommons.lsu.edu/gradschool_theses



Part of the [Animal Sciences Commons](#), and the [Molecular Genetics Commons](#)

Recommended Citation

Haynie, Taylor, "RECOMBINANT DNA VACCINE DESIGN AS A POTENTIAL STRATEGY AGAINST BOVINE FOOT AND MOUTH DISEASE VIRUS (FMDV)" (2023). *LSU Master's Theses*. 5772.

https://digitalcommons.lsu.edu/gradschool_theses/5772

This Thesis is brought to you for free and open access by the Graduate School at LSU Digital Commons. It has been accepted for inclusion in LSU Master's Theses by an authorized graduate school editor of LSU Digital Commons. For more information, please contact gradetd@lsu.edu.

RECOMBINANT DNA VACCINE DESIGN AS A POTENTIAL STRATEGY AGAINST BOVINE FOOT AND MOUTH DISEASE VIRUS (FMDV)

A Thesis

Submitted to the Graduate Faculty of the
Louisiana State University and
Agricultural and Mechanical College
in partial fulfillment of the
requirements for the degree of
Master of Animal Sciences

in

The School of Animal Sciences

by

Taylor Michelle Haynie
B.S., Louisiana State University
May 2023

This thesis is dedicated to my parents, Dr. Stacia Haynie and Scott Haynie, without whom I would not have the ability or confidence to pursue my aspirations.

You is kind. You is smart. You is important.

- Aibileen Clark

DreamWorks, *The Help*

Acknowledgments

I would like to recognize Dr. Richard Cooper, who provided me with an opportunity of a lifetime to work under his expert guidance and set the foundation for my future career. His constructive guidance, expertise, and incredible leadership throughout the thesis process made it possible to not only have the confidence to complete a thesis but to defend among esteemed colleagues and peers. Specifically, the impact on my academic experience has continually expanded my ability to critically problem solve and instilled a stronger sense of confidence in myself that will guide me long after my academic endeavors. His continual encouragement and guidance are not only invaluable but has made me the person I am today. For that I am forever grateful.

I would like to acknowledge my remarkable committee members, Dr. Philip Elzer, and Dr. Vinicius Moreira for their scholarly contribution and their teaching prowess not only from the intensive activities and obligations of being a part of a committee but the integral role they play in sustaining the College of Agriculture's academic enterprise.

Thank you to the College of Agriculture for its commitment to academic rigor and for making sure their students are given everything they need to ensure their work is of highest quality and standard. I am honored for their scholarly contributions and helping me achieve a deeply important milestone of my academic career and solidifying an essential step towards my future professional life. I would like to thank Sue Hagius for all her guidance and expertise with my experiments and always there for any questions or problems that we needed help with. I'd like to thank Thaya Stoufflet with the Gene Lab at the LSU School of veterinary Medicine. I would also like to give a special thanks for the technical support and expertise of fellow colleagues and cohorts, Ashley Edwards, Stephanie Korle, and Mack Solar for your active

participation in my experiments and acting as incredible mentors during my academic journey. Thank you to Alexis Nguyen for your lifelong friendship and support throughout this entire journey not just in the bounds of academia but outside as well. I would like to especially thank my dear friend, Ashley Edwards, whose assistance and support made this academic journey possible. Her moral integrity, genuine compassion, and unwavering support, met with an assiduous work ethic, and intuitive thinking make her not only a remarkable scientist but a wonderful person. It is with the utmost conviction that regardless of where my academic endeavors take me, if I can emulate even a fraction of Ashley's character, I will accomplish great and beautiful things.

Lastly, I would like to convey my deepest gratitude towards my parents, Scott and Stacia Haynie, who have not only supported but encouraged me throughout this entire process. I am forever in your debt (literally and figuratively) and would be nothing of who I am today without your unconditional love, faith, and capacity to never give up on me.

Table of Contents

Acknowledgments.....	iv
Abbreviations	xi
Abstract	x
Chapter 1. Introduction	1
1.1. Taxonomy and Nomenclature.....	1
1.2. Genome Organization	4
1.3. Virus Life Cycle.....	5
1.4. Induction of Innate Immunity	8
1.5. Transmission and Clinical Signs.....	9
1.6. Control and Treatment	11
1.7. Detection and Serological Testing	13
1.8. Vaccination	15
1.9. Optimization of DNA Components	16
1.10. Justification and Hypothesis	21
Chapter 2. Materials and Methods	24
2.1. Vaccine Construction.....	24
2.2. Transformation and Cloning.....	29
2.3. Cells and Transfection	32
2.4. Optimized Serological Testing	36
Chapter 3. Results	40
3.1. Verification of Vaccine Size and Placement	40
3.2. In Vitro Results	45
3.3. Discussion.....	48
3.3. Conclusion	51
Appendix A.....	67
A.1. Experimental Data.....	48
A.2. Protocols	51
References.....	58
Vita.....	67

Abbreviations

FMDV	Foot-and-mouth disease virus
FMD	Foot-and-mouth disease
DNA	Deoxyribonucleic acid
ICNV	International Committee on Nomenclature of Viruses
ICTV	International Committee on Taxonomy of Viruses
ssRNA	Single-stranded ribonucleic acid
HT-NGS	High-throughput next-generation sequencing
ERAV	Equine rhinitis A virus
BRAV	Bovine rhinitis B virus
SAT	South African Territory
WLRFMD	World Reference Laboratory for Foot-and-Mouth Disease
ORF	Open reading frame
Kb	Kilobase
Nt	Nucleotide
NSP	Nonstructural protein
L^{PRO}	Leader protease
VPg	Viral genome linked protein
Rpdp	RNA-dependent RNA polymerase
UTR	Untranslated region
NCE	Noncoding element
IRES	Internal ribosomal entry site
Pk	Pseudoknot
HS	Heparan sulfate
eIF	Eukaryotic translation initiation factor
PTBP	Polypyrimidine tract binding protein

SP	Structural protein
SER	Smooth Endoplasmic reticulum
PRR	Pathogen recognition receptors
PAMP	Pathogen associated molecular pattern
MHC	Major histocompatibility complex
IFN	Interferon
TLR	Toll-like receptor
RLR	Retinoic like receptors
MDA5	Melanoma differentiation-associated gene
VP	Viral protein
PCP	Progressive Control Pathway
LMIC	Low-and-middle-income countries
VAC	Vaccine antigen concentrate
PIADC	Plum Island Animal Disease Center
FAO	Food and Agriculture Organization
NAFMDVB	North American FMD Vaccine Bank
USDA	US Department of Agriculture
APHIS	Animal and Plant Health Inspection Service
DIVA	Differentiating infected and vaccinated animal
OIE	World Organization for Animal Health
WHO	World Health Organization
CMV	Cytomegalovirus
DC	Dendritic cell
SV40	Simian virus 40
NLS	Nuclear localization Sequence
MIP-1 α	Macrophage inflammatory protein-1 alpha
BGH polyA	Bovine growth hormone polyadenylation

FRS	Free rotational spacer
NCBI	National Center for Biotechnology Information
IEDB	Immune Epitope Database and Analysis Resource
IDT	Integrated DNA Technologies
SB AMP	Super Broth Ampicillin
DMEM	Dulbecco's Modified Eagle Medium
DPBS	Dulbecco's phosphate buffered saline
FBS	Fetal bovine serum
ELISA	Enzyme-linked immunoassay
Ig	Immunoglobulin
PCR	Polymerase chain reaction
RT-PCR	Reverse transcription-polymerase chain reaction

Abstract

Foot-and-mouth disease virus (FMDV) is the causative agent for foot-and-mouth disease (FMD) that infects primarily cloven-hoofed animals, the majority of which are domesticated cattle and other important livestock. FMD is highly transmissible and found in all secretions and excretions of infected animals. North America, Europe, and Australia have successfully eradicated the virus with the help of a well-defined fiscal infrastructure and access to successful control measures. Less developed regions, including many Asian and African countries, have maintained an endemic status for decades. African territories are of particular concern because of the indigenous African Buffalo population that serves as an important FMDV reservoir. Incursion of FMDV among livestock herds leads to a precipitous decline in productivity and causes irrevocable economic hardships to these farmers. Once an outbreak has occurred, international trade of livestock and animal product exports are prohibited, further devastating the economy. Control of FMDV in endemic regions must include reliable diagnosis through differentiation between infected and previously vaccinated livestock, access to limited emergency vaccine resources, proper sanitary methods including farm biosecurity and quarantining and culling of infected livestock. Existing FMD vaccination includes killed or inactivated and synthetic proteins that offer only short-term immunity and require repeated booster and adjuvant administration. Other challenges with this vaccine platform include a lack of cross-protection against multiple strains, the need for a cold storage, and the risk of reinfection in previously protected livestock due to short-term immunity. To overcome these challenges, the research utilized recombinant DNA technology to produce a safer and cost-effective vaccine. Prior research demonstrates that the structural proteins of the virus exhibit immunogenic potential through capsid stability, antigen binding, and multi-epitope formation. Using this

information, a plasmid-based vaccine expressing a multi-epitope protein was designed with a composite of the major FMDV antigens defined in the literature. This model offers a potential multi-epitope DNA based vaccine design as a cost-effective and non-pathogenic alternative for the protection against FMD. If successful, vaccinated animals could be differentiated from infected animals using an optimized specific diagnostic assay for antibody detection. The design, construction, and initial testing of the vaccine are discussed.

Chapter 1. Introduction

1.1. Taxonomy and Nomenclature

The causative agent for Foot and Mouth Disease (FMD) is the Foot and Mouth Disease Virus (FMDV), a species within the genus *Aphthovirus* of the family *Picornaviridae* [1]. Historically, based on records dating back as early as the 16th century, FMDV was the first disease-causing pathogen in animals to be identified as a virus [2]. The virus infects cloven-hoofed animals, such as cattle, pigs, sheep, and goats. It has also been reported in at least 70 wild species, particularly the African buffalo, which serves as an important maintenance host. *Picornaviridae* is the largest genera of viruses, including *Enterovirus*, *Parechovirus*, *Hepatovirus*, *Rhinovirus*, and *Aphthovirus* [3]. They are accountable for prototypical diseases such as the common cold, meningitis, and FMD [4]. The initial International Committee on Nomenclature of Viruses (ICNV) founded in 1966 classified genera based on morphology, physicochemical properties such as particle size, molecular mass, buoyant density, and pH stability [5, 9]. The Baltimore Classification of viruses was later established in the early 70s and used in counterpart with the now recognized International Committee on Taxonomy of Viruses (ICTV) to partition viruses based on the type of nucleic acid and mode of replication. [6,7,8]. Picornaviruses are non-enveloped, positive-sense, single-stranded ribonucleic acid ((+) ssRNA) virions encased in a densely packed pseudo (T=3) icosahedral procapsid structure with a diameter of 20-30 nanometer (nm). The FMDV procapsid initially begins with the assembly of four protein monomers, VP1, VP2, VP3 exposed on the surface and VP4 facing internally,

forming a protomer (60 copies) and used for the arrangement of the capsomere (pentamer) structure (12 copies) that will make up the procapsid surrounding the naked genomic RNA [4].

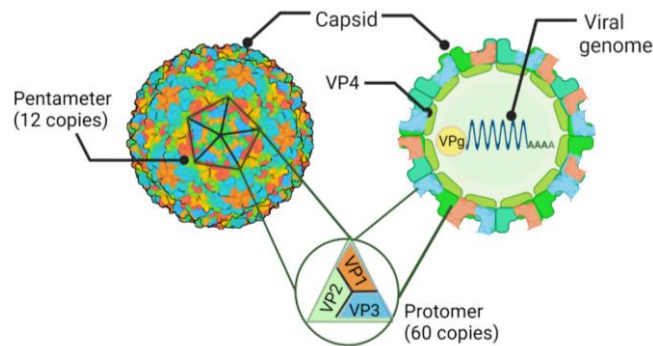


Figure 1.1. Schematic representation for the biological assembly of wild type of FMDV-O. On the left is a 3D experimental data snapshot of a wild type FMDV-O aggregated particle (VP4 and viral genome not visible) after complete icosahedral assembly. The primary citation for identifying this experimental protein structure is 7ENP retrieved from the Protein Data Bank (PDB). On the right is a 2D cross section of a FMDV particle where VP4 and the viral genome are visible. (Made with Biorender)

Over the past decade, high-throughput next-generation sequencing (HT-NGS) technologies have vastly expanded how scientists investigate evolutionary relationships between nucleotide sequences [11]. Until recently, FMDV has been the only prototypical species for *Aphthovirus*, but new strains of Equine rhinitis A virus (ERAV) and Bovine rhinitis B virus (BRAV) have been classified as *Aphthovirus* [9]. Further classification of FMDV using serological testing established seven distinct serotypes: A, O, C, SAT1, SAT2, SAT3, and Asia 1, each immunologically distinct from one another [12]. The first two serotypes to be recognized in 1922, Vallée A (FMDV-A) and Vallée O (FMDV-O), were named after Vallée, the scientist who distinguished them, and after the department of Oise in France and Allemagne, where they originated [17]. The next serotype to be determined, Waldmann C (FMDV-C), was named after the scientist who initially identified three versions of the serotypes A, B, and C [18]. However, only FMDV-C was accepted as a distinct serotype. FMDV-C is currently not known to be in

circulation anywhere globally [19]. The next three serotypes were discovered in southern African territories, given the abbreviation SAT, distinguished by 1, 2, and 3 (FMDV-SAT1, FMDV-SAT2, FMDV-SAT3). The last serotype, Asia-1 (FMDV-Asia-1), was named after Pakistani and Indian origins [20]. Serotypes are further grouped based on similar geographical locality between genetically distinct strains, known as topotypes. Currently, there are eight distinct topotypes designated as Middle East-South Asia (ME-SA), South-East Asia (SEA), Cathay, Indonesia-1, Indonesia-2, East Africa, West Africa and Europe-South America (Euro-SA). FMDV-O has the highest number of recorded occurrences among all topotypes with FMDV-Asia-1 outbreaks rare and FMDV-C nonexistent [4, 21, 22].

Phylogenetic analysis using prototypical FMDV isolates from each serotype indicate the genomes share 80-85% nucleotide sequence identity [15]. The lack of identity shared between sequences is attributed to the VP1 coding region. Only 50-70 % nucleotide sequence identity of VP1 is conserved across all serotypes [16]. The variability is attributed to a mutation on the G-H loop of the VP1 coding region involved with viral attachment and host cell entry [12]. The variation within the G-H loop structure is caused by the viral replicase's lack of proofreading repair activity [4]. This phenomenon is why the RNA sequences of the VP1 region are most used for phylogenetic analysis, genetic characterization of strains, and even aiding epidemiologists in tracing outbreak origins for FMD [16]. The World Reference Laboratory for Foot-and-Mouth Disease (WLRFMD) recommends writing out the name for a specific isolate first by serotype then by topotype abbreviation followed by lineage (each classification written with a forward slash (/) and with any sub-lineage written as a superscript at the very end [22].

3' UTR region (90 nts) poly (A) tail. Covalently linked to the 5' UTR is VPg^{1,2,3} ranging in 24 to 25 amino acid residues in length [23, 24]. Picornaviruses normally process only one copy of the VPg while FMDV processes three copies of VPg^{1,2,3}, an attribute theorized to greatly increase virulency [25].

The 5' UTR of FMDV is described as consisting of highly functional noncoding elements (NCEs) including a S fragment, a conserved poly C tract, a various number of pseudoknots (pks), and finally an internal ribosomal entry site (IRES) made up of conserved stem loop structure motifs [26, 27]. The exact functions of NCEs within the UTRs are not fully understood but have demonstrated importance for efficient viral replication within the host cell [28].

1.3. Virus Life Cycle

In general, it has been observed that cellular receptor homologs across different species cannot be interchangeable for supporting FMDV infection [29]. In bovine species, FMD pathogens exhibit tropism for cell specificity. FMD virions can enter the epithelial cell one of two ways, Hairpin (HS)-mediated endocytosis or integrin-mediated endocytosis [30]. One study demonstrated that nearly all FMD virions use integrin receptors to commence endocytosis into the host cell except FMDV-O particles which exclusively use HS to mediate endocytosis [31].

Integrin-mediated endocytosis allows for viral attachment with any of the four integrin receptors, avB1, avB3, avB6, and avB8, located on the host's cell surface [32, 33, 34, 36]. While the exact function of each integrin receptor remains unknown, FMDV can bind with more integrins than any other Picornavirus [37]. The avB6 integrin is a special cellular receptor only found on epithelial cells of the oral cavity, upper respiratory tract, pharyngeal tissue, gastrointestinal tract lining and the coronary bands between hooves for cloven hoofed species

[36]. It has been previously determined that avB6 restricts which type of cells FMDV can infect and freely replicate [35].

The integrin receptors are attached to adaptor protein complexes located in between the lipid membrane of the host's cell [36]. Binding of the antigen to the integrin receptor signals the release of clathrin, a naturally occurring molecule within the cytoplasm to aid in endocytosis [36, 37]. Clathrin attaches to the adaptor protein complexes which creates a clathrin coated pit then eventually a vesicle around the virion. Once internalization is complete, the now fully clathrin-coated vesicle is now an endosome allowing mobilization of the virus within the cytoplasm.

Virions within FMDV-O that enter through HS-mediated endocytosis use naturally occurring proteoglycans, heparan sulfates (HS), located between the cholesterol-enriched membrane to facilitate attachment. After successful antigen binding to HS, caveolin-1 receptors found within the cytoplasm are signaled to adhere to the cholesterol-enriched membrane forming a caveolin coated vesicle then eventually an endosome surrounding the virion [37].

FMD virions exhibit unique sensitivity to acidic environments becoming completely unstable at pH levels lower than 6.8. The newly formed endosome generated from either pathway has a relative pH of 6.0 [9,10]. The tightly packed capsomeres that surround the genome are triggered to be dissimilated due to the relatively acidic environment within the endosome. The low pH levels ensure that the outer capsid will be chemically stripped and broken apart allowing for naked genomic RNA to be translocated from the endosome into the cytosol [37]. Instead of capping the 5' end of the mRNA to initiate translation, FMDV has genomic RNA with positive polarity that uses its own IRES to drive translation and allow for intrinsic infection [38].

In eukaryotic organisms, a protein complex formed by scaffold proteins including eukaryotic translation initiation factors (eIF4G, eIF4A, eIF4E), polypyrimidine tract binding

protein (PTBP), multimeric factor (eIF3), and small ribosomal subunit (40S) recruit the 5' cap structure of the mRNA for protein synthesis to take place. By contrast, FMDV lacks the 5' cap structure and instead auto-cleaves the L^{PRO} which interacts with the PTBP on the cell's protein complex removing eIF4E binding sites, consequently inhibiting host cap-dependent translation [24, 39]. After L^{PRO} initiates viral translation, L^{PRO} also cleaves the remaining P1 region of the initial polyprotein precursor structure into capsid SP intermediates, VP0, VP3, VP1 and one NSP, 2A. Once 2A is cleaved, this NSP then acts as a proteinase cleaving VP0 giving into VP4 and VP2. This step will conclude the maturation of the final SPs. 2A is then tasked with cleaving the P2 region into mature NSPs, 2B and 2C. 2A is also responsible for cleaving P3 intermediates, specifically $3C^{\text{PRO}}$. The $3C^{\text{PRO}}$ processes the remaining P3 intermediates for the maturation of the remaining NSPs, specifically $\text{VPg}^{1,2,3}$ (3B) and $3D^{\text{POL}}$ [40]. Once the three copies of VPg are generated, they become covalently linked to the beginning of the 5' UTR acting as the uridylation site necessary for priming RNA synthesis. The induction of the $\text{VPg}^{1,2}$ uridylation site signals the cleavage of the Rpdp, $3D^{\text{POL}}$ to carry out RNA synthesis [41]. The $3D^{\text{POL}}$ enzyme with the assistance of NSPs 3A, 2B, and 2C is responsible for the replication of FMDV RNA. Viral replication has been observed to take place quickly and efficiently on the surface of host cell organelles such as the smooth endoplasmic reticulum (SER) and the Golgi apparatus [38]. Encapsidation then occurs when the naked viral genomic RNA synthesized from every replication cycle is released into the cytosol triggering auto-assembly of the mature translated SPs around the virion until it is fully encapsulated. The host cell is then lysed, and the newly assembled virions are released to retrieve their next host [12].

1.4. Induction of Innate Immunity

Despite advancements in preventative and treatment strategies including novel vaccines, strict biosecurity measures and routine immunizations, FMD remains one of the greatest threats towards livestock within the agricultural industry, especially, dairy and beef cattle production. A more in-depth and comprehensive review of bovine immunology has allowed scientist to better understand how these pathogens are able to circumvent host immune functions and how the knowledge of this will aid in optimizing current anti-FMD strategies that could greatly reduce the vulnerability towards the disease and maintain cattle health.

The hosts' immune system is committed to the protection of organisms against foreign body invasions and promoting tissue repair after injury. Multiple lines of defense are strategically deployed by the host at different stages of infection, each more intricate than the last [48, 49].

The first line of defense relies on the hosts' innate immune system built around intricate chemical and physical barriers set in place to prevent a pathogen from gaining entry and prevent viral replication [48, 50]. Just like other animals, cattle's first line of defense towards invading pathogens uses physical barriers such as epithelial cells and mucosal membranes lining the respiratory tract and defense mechanisms such as coughing and sneezing to clear the virus. The primary site of infection FMDV is restricted to epithelial cells of the nasopharyngeal mucosa where viral load is amplified then is carried through lymphatic-associated tissues to further replicate. The innate immune response begins as the virions interact directly with the epithelium cells either through lytic infection of the cells or phagocytosis. Pathogen recognition receptors (PRRs) released from the host cell identify pathogen associated molecular patterns (PAMPS) from the virus and that mutual interaction is essential for activating the immune response [12, 51,52]. After PRRs and PAMPS initial interaction during the local response, NK (Natural Killer)

cells release interferons (IFNs), chemokines, and inflammatory cytokines to eliminate pathogens and clear the virus. Specific PRRs involved with viral detection include Toll-like receptors (TLR) and retinoic acid-inducible gene I (RIG-I) like receptors (RLR) [55]. RLRs can be further classified into two groups, RIG-I and melanoma differentiation-associated gene (MDA5) [12, 55]. RLRs such as MDA5 are important during an FMDV infection because they play an important role for inducing an immune response specifically against RNA virus infections. A recent report determined the viral 3C^{PRO} inhibits MDA5 expression to evade the immune response of the host and gain entry within the host cell [55]. TLRs are found on the endosomal surface of macrophages, dendritic cells (DCs), and other innate immune cells [52]. NSPs, 2B and 2C of FMDV have also shown to increase plasmatic membrane permeability into the host cell by blocking protein degradation pathways of the innate immune system [56]. L^{PRO} also compromises the host's ability to develop an antiviral response since L^{PRO} inhibits the host cell's ability to carry out cap dependent translation. FMDV can inhibit toll like receptor pathways on DCs and as macrophages that reduce also reduce the MHC II ability to present antigens to the T cell. The inhibition of TLS also stimulates the DCs to increase IL-10 protein in response which reduces the expression of MHC-1 and in turn decreasing the adaptive immunity of the T cell to effectively activate the humoral immunity and induce effective neutralizing antibodies to promote viral clearance.

1.5. Transmission and Clinical Signs

The principal routes for transmission of FMD in bovine is via aerosolization entering through the pharyngeal mucosa and associated lymphoid tissues of the upper respiratory tract replicating at the site of infection. Initially, during the acute phase the virus, FMDV SP and NSPs can be detected in the epithelial cells of the nasopharyngeal mucosa for 1 to 3 days. From

there, the virus travels through the lymphatic system circulating within the blood for up to 3 to 5 days replicating in the epithelium of the mouth, muzzle, teats and feet.

Within 24 hours of entering the acute phase of infection, all secretions and excretions can become infectious. The virus can also enter through ingestion of contaminated feed or water as it is shed through all secretions and excretions of acutely infected organisms. Human care takers can also contribute to the transmission of the disease, as they can serve as mechanical vectors for up to 48 hours. The entire infection process is not only self-efficient but extremely fast. It has been determined that it takes approximately one hour for any modification or chromatin condensation after initial infection to occur [43]. By the sixth hour, the life cycle of the virion is complete and looking for a new host to infect. Within 48 hours, physical signs will start to appear including ruptured vesicles and lesions leading to chronic lameness and reduced milk yield in dairy cows. The average incubation period lasts about 14 days in cattle and roughly a week in other domestic livestock [4].

The significant amount of stress and discomfort caused by FMD results in a major reduction in livestock production such as reduced milk yield or even permanent depletion in milk production after infection [4, 12]. Unprocessed meat and milk can also serve as a mechanical vector for transporting the disease. Morbidity reaches 100% in susceptible populations where contact is imminent, such as a herd. Conversely, mortality rates are less than 1 % with deaths mostly seen in calves [4]. There can be sudden relapse of the malignant form of the disease that can result in cardiac failure leading to dyspnea and death. There are also reports of still births or abortions that accompany these symptoms with full recovery ranging anywhere from 8 to 10 days [44].

1.6. Control and Treatment

Due to the highly contagious and aggressive nature of the virus, infected meat and milk cannot be exported to FMD-free countries such as the United States or the European territories [45]. Introducing this pathogen into an FMD-free region is considered agroterrorism as it would be devastating to any economy and would be almost a decade before any country could recover or gain that FMD-free status again [46]. FMD status is divided into five categories, (1) being those countries that can exhibit a FMD free status and (5) with the highest prevalence. Those countries with FMD free status or category (1) have experienced no incursions within the last five years. Category (2) refers to regions that experience geographically contained outbreaks with reliable reporting episodes only one to three times within a five-year period. Category (3) exhibit erratic frequency of FMD outbreaks and inconsistent and unreliable reports in the past five years. Category (4) is given when the countries exhibit persistent infection to the point where disease becomes a seasonal hazard but restrict potential spread of disease to neighboring regions. Category (5) is reserved for countries exhibiting high incidence of FMD occurrence throughout the year and remains endemic. Serotypes exhibit some topology with serotype O occurring more than any other serotype followed by Asia 1 [47]. The status of countries on the Progressive Control Pathway for FMD (PCP-FMD) is evaluated according to defined criteria [58, 59]. Countries with endemic disease are in stages 1 to 3 including Africa and Asia territories while FMD-free countries are in stage 4 and above such as North America, Europe, and Australia which have successfully eradicated the disease. Low-and-middle-income countries in Africa (LMICs) such as Zambia and neighboring countries including the Democratic Republic of the Congo and Tanzania are currently at Stage 2 [61, 62]. Tanzania was ranked the second largest source of livestock in Africa, with over 30 million cattle alone and accounting for over 70% of yearly revenue. In research from Häsler and others a statistical model was designed to analyze the cost-benefit of establishing FMD-free zones in areas like Zambia where the disease

is prevalent, and livestock is a main source of revenue [64]. The benefit of eliminating the disease would ensure the export of cattle and other animal by-products and allow the imported livestock to not risk contamination. The lack of available control measures and endemic status by the PCP-FMD prevents international trade for these regions and are prohibited from importing FMDV vaccines because this pathogen can maintain virulence for in well shaded and cool areas for up to six months making meat and dairy products an unfortunate maintenance host [63].

While the United States (US) have maintained FMD-free status since the early 1900's, the national government has gone to great lengths and heightened safety measures to ensure FMD remains a foreign animal disease. Until recently, FMD vaccine banks consisting of vaccine antigen concentrate (VAC) were prohibited on North American territory. The only research facilities with access to vaccine banks included Plum Island Animal Disease Center (PIADC) and the Food and Agriculture Organization (FAO) FMD World Reference Laboratory at Pirbright Institute in the United Kingdom. In 2018, after the Agricultural Improvement Act was passed by Congress, the PIADC was dissolved and reestablished on the US mainland as the North American FMD Vaccine Bank (NAFMDVB) with the only access to FMDV vaccine antigen concentrates (VAC) for select antigen exclusion [63]. In accordance with the US Department of Agriculture Animal and Plant Health Inspection Service (USDA APHIS) and Department of Homeland Security Science and Technology Directorate (S&T), Boehringer Ingelheim was approved for a conditional license to manufacture a vaccine with the use of an inactive, wild-type Ad5-Vaccine [65]. This high-potency adenovirus-vectored vaccine is the only licensed vaccine by the USDA during the event of an emergency in the United States. [66]. In other FMD-free regions, contingency plans involving vaccination are only distributed to neighboring regions where outbreaks are occurring and access to it is restricted by the World

Organization for Animal Health (OIE)¹ [47]. Normally, vaccine quality control is determined by the producer and vaccine batches are only released when they pass the quality control parameters. However, lack of maintenance of the cold chain before, during, or after transport and/or importation may reduce the vaccine efficacy even if the vaccine initially contained a sufficient payload of serotype(s). The immune response towards FMD once given the vaccine provides short-term protection ranging from seven to twenty days. Current live attenuated vaccines must remain chilled throughout the administration process to not destroy the RNA within the vaccine. If an outbreak were to occur in a herd and vaccination was available, the first step would be to treat all susceptible species along with booster vaccination during outbreak to help warrant containment and long-term immunity [65]. Although cattle might be vaccinated, a major issue is that animals can still be infected (known as a carrier with no physical symptoms) and can easily cause an outbreak in herds and other species. For natural infection, cattle that test positive for FMD also test positive for vesicular stomatitis while in some rare cases also positive for Bluetongue. Pigs that test positive for FMD also exhibit vesicular stomatitis, vesicular exanthema of swine and swine vesicular diseases. For sheep and goats who test positive for FMD, vesicular stomatitis can be present as well but isn't always a determining factor whereas sheep and goat with Bluetongue is a determining factor. For this species, vesicular stomatitis is present without FMD, and all other major determining diagnoses are not common [66].

1.7. Detection and Serological Testing

Current FMD vaccines commercially available as well as potential vaccine platforms must be approved for differentiating infected and vaccinated animals (DIVA). DIVA allows the potential for vaccinated animals to not be inaccurately diagnosed and slaughtered. DIVA uses

¹ The OIE was abbreviated for the Office International des Epizooties but later changed its name in 2003 to World Organization for Animal Health. They retained the original abbreviation though [47].

specific FMDV NSPs for serological testing to detect if infection is present. Whereas a natural infection induces antibodies for specific NSPs (2C, 3A, 3B, 3C) only present during viral replication within the host cell, those same NSPs are completely absent from clarified virus stocks used for vaccination. DIVA serological testing can also be used to differentiate potential carrier convalescent animals from vaccinated livestock in both cattle and swine. No test has 100% sensitivity or specificity but combination serological testing using multiple NSPs in one assay including the commercially available FMDV 3ABC ELISA offers the highest specificity and sensitivity for the presence of infection, regardless of the animals' vaccination status [67].

Distinguishing infected animals from vaccinated is a tedious, expensive and a control measure not feasible in lower socioeconomic regions. In endemic regions without access to Ad5 emergency vaccine or DIVA testing, culling the entire herd is the only successful control method to eliminate all clinically infected animals as well as those who aren't clinically infected but could be carriers for potential infection. There also is strict restriction of animal movement outside of infected premises, proper carcass disposal and environmental disinfection. Current management the farmers and livestock owners should take depends on the cleanliness and hygiene measures taken with their herd [68]. The virus occurs primarily as an outbreak within a herd, so once infected, movement, handling, and any physical contact should be virtually eliminated, strict quarantines set in place as well as proper carcass disposal and environmental disinfection. What makes FMD particularly resistant is its' ability to withstand treatment with common disinfectants. For drinking water, sanitized water should be used and all equipment, clothes, hair, and other items that have contacted infected hosts should be thoroughly washed with industrial soap or 4% sodium carbonate [69]. Veterinarians, farmers, and handlers who encounter any infected animal can serve as mechanical vectors physically carrying the disease

from one host to another. These tedious control measures are not practicable long-term. There is a need for a non-pathogenic vaccine for protection against FMDV that can be mass-produced and easily administered in endemic regions, especially when commercially available vaccines are not an option and hygiene measures are limited [70].

1.8. Vaccination

Recombinant DNA vaccines offer many benefits that other vaccine approaches lack. For economically developing, endemic countries, the benefits that matter most are the safety and the required storage requirements for DNA vaccines. The Ad5-Vaccine is the only vaccine platform approved in the state of an emergency outbreak. This adenovirus-vectored vaccine is killed and does not provide cross protection against other serological strains so multi-valent vaccines are required as several strains may be active at the same time. Vaccination only offers short term immunity lasting six months and vaccinated animals can be sub clinically infected meaning the animal is now a carrier presenting no clinical signs and only replicating the virus within the nasopharyngeal tissue.

Differentiation of infected versus vaccinated animals DIVA uses NSP ELISA to detect if infection is present. Natural infection induces antibodies for NSP involved with virus replication where the vaccine does not.

The currently available live-attenuated vaccine has the capability to revert to a virulent phenotype [69]. Recombinant DNA vaccines cannot do this as they do not contain the virus itself. Also, DNA can be stored at room temperature for up to a year, provided it is in a sterile environment. This is particularly helpful to these countries, as access to cold storage is limited or non-existent.

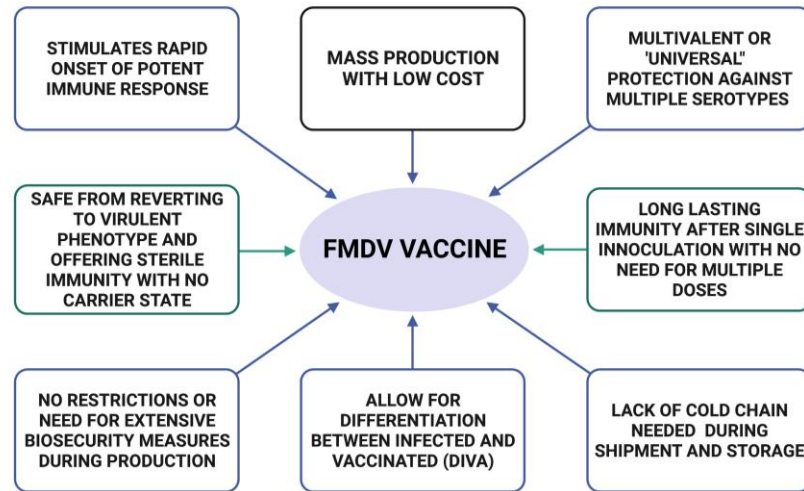


Figure 1.3. Optimal parameters for vaccine to effectively eliminate and eradicate FMD. (Made with Biorender)

Vaccinations are an effective method of disease control, as they can contribute to the prevention and suppression of FMD epidemics. There is a need for inexpensive and easily delivered vaccine options in regions that do not currently qualify for the commercially available vaccines. The ideal parameters for a vaccine with no specification on type of vaccine but what features are necessary for optimal success can be stated in Figure 1.3. This DNA vaccine platform designed and constructed today is a potential option for meeting many of those requirements and providing protection for livestock and the economic development that can flow from it [70].

1.9. Optimization of DNA Components

The concept of plasmid DNA vaccines are transfecting cells with specific-antigen DNA sequences to induce a robust immune response. DNA vaccines have low transfection efficacy, easily being degraded preventing that immune response from mounting that result in low therapeutic efficiency. The encoded antigen DNA must not only enter the cell but pass through the nuclear membrane for transcription to occur which then can now be processed into antigen-derived peptides. Peptides are loaded onto MHCI molecules internally that activate CD+8T cells

induce the priming of B cells necessary to carry out a humoral immune response. For the CD8 +T cells to be fully activated, they will need the assistance of helper CD4 + T cells which are exclusively activated by the loading of MHCII molecule. MHCII molecules are specific to exogenous antigens meaning antigen-derived peptides must be able to load in chorus to both MHCI and MHC II in order to active a full immune response. DC are highly professional APCs and that can load both molecules in parallel and under the right conditions. Specialized APCs like DCs also dictate specificity of the immune response and particularly susceptible to transfection of gene-based vaccines *in vivo*.

Optimization in the immunological parameters of the DNA vaccine design has consistently demonstrated substantial improvements in delivery, humoral and cell mediated responses and enhanced protection. Specifically, with FMDV, DNA plasmids encoding the VP1 empty capsid including NSPs, 2A and 3C^{PRO} have proven its success in recent research presenting immunodominant properties and eliciting a higher cellular immune response against specific serotypes [54, 71]. Other essential components necessary to combat the lack of transfection rate and short-lived immune response include a promoter, adjuvant, optimized codon, a nuclear localization sequence, optimal environment for transfection, and precise serological testing.

1.9.1. Promotor

The cytomegalovirus (CMV) promoter was proven to have broader and higher immunity induction when compared to other promoters expressing recombinant proteins. Moulin et al. focused on promising promoters to see which is most favorable for driving antigenic expression and DC-specific activity. CMV proved to direct a high level of transient gene expression in multiple cell-type settings. The SV40 and CMV promoters yielded the largest fractions of green

fluorescent protein (GFP) positive cells [72]. Although aspects of nuclear transport occur within the ORF, most of the transport activity resides in the CMV Promoter and enhancer region within the cell [73]. The CMV constitutive promoter showed consistent transcriptional activity in multiple types of cell lines and vectors making this element an essential component to the overall DNA vaccine design.

1.9.2. Nuclear Localization Sequence

The simian virus 40 (SV40) nuclear localization sequence (NLS) mediates nuclear translocation of recombinant DNA into the protein [74]. The SV40 enhancer facilitates maximal transport and nuclear uptake of plasmids. The CMV alone cannot drive expression but placed together with the SV40 NLS has proven in previous studies to contribute greatly to the nuclear transport of plasmids for gene expression. The SV40 sequences on the 5' end of the CMV promoter has been previously determined to be essential for nuclear transport of plasmids to gene expression [75].

1.9.3. Signal Sequence

Macrophage Inflammatory Protein-1 alpha (MIP-1 α) is a 92 amino acid protein that contains a 22 amino acid residue signal sequence involved in the secretion of the mature protein from the cell. The MIP-1 α signal sequence is a derivative of the chemotactic cytokine from the subfamily of chemokines secreted by a variety of immune cells including macrophages, NK cells as well as T cells. in cytokines [76], which are secreted by dendritic cells [77]. These cells play a direct role with activation of macrophages, used by NK cells to aid CD8⁺ T cells during the antigen-presenting phase as well as aiding Th1 cells to recognize and eradicate future infections. [78]. A bovine-specific MIP-1 α signal sequence exists and directs the secretion of cytokines from dendritic cells and has proven to be efficient with *in vivo* transfection [79].

1.9.4. Adjuvant and Optimized Codons

Adjuvants have shown to play an important role in vaccine design and elicit a higher cellular immune response than without, especially against more complex viruses such as FMDV [80]. Plasmid DNA vaccination encoding a genetic adjuvant such as Th1 cytokine, IL-18, can help modulate the direction and strength of antigen-specific cellular and humoral immune response in vivo. The inclusion of an adjuvant induces and regulates delivery of antigens to APC. The swine IL-18 adjuvant has shown specific T cell response specific to FMDV. A group of scientists utilized the FMDV genome region P1-2A capsid protein along with the 3C protease gene of FMDV types of Asia-I and O along with a genetic adjuvant [81]. The genetic adjuvant that they used was the swine IL-18 gene. Upon testing their vaccine against the commercial vaccines, they found that their vaccine mounted a T cell response specific to FMDV.

Codon optimization was performed to potentially increase the efficiency of protein expression of the vaccines within our target cell line. The amino acid sequence of the wild-type viral proteins expressed by the DNA vaccine are compared to those sequences from the same vaccinated host species. Codons (triplet of base pairs) with high frequency for gene expression found within the vaccinated species are used to replace codons in the DNA vaccine that show low frequency. The entire amino acid sequence of the DNA vaccine remains the same while only altering the codons for optimal protein expression. There has been conclusive research that shows codon optimization has a direct effect on translation efficiency.

1.9.5. Polyadenylation Signal Sequence

A polyadenine tail is needed to protect the 3' end of the protein secreted from the dendritic cell, and to produce a polyadenine tail, a polyadenine signal sequence is required. The bovine growth hormone polyadenylation (BGH polyA) signal was reported twice as efficient as the SV40 polyA signal sequence in producing a polyadenine tail [82].

1.9.6. Free Rotational Spacers

The inclusion of Free Rotational Spacers (FRS) is a small yet extremely important constituent when designing recombinant vaccines [83]. FRS are synthetic spacers made up of small discontinuous sequences engineered to mimic natural interaction between immunodominant epitopes or protein domains. FRS allows proteins to fold freely and form the correct three-dimensional structures while also improving stabilization [84]. A group of researchers that have used FRS found that they greatly decrease binding affinity between the core binding regions thus joining the epitopes [85].

1.9.7. Cells and Transfection

Transfection is a process of introducing foreign nucleic acids into eukaryotic cells and is a popular method for studying protein expression [86]. In recent years, technological advances have expanded applications and selection methods for transfection [87]. Today there is a wide range of technologies allowing for the delivery of DNA into the cytoplasm.

Transfection can be separated into two types. There is stable transfection which is ideal for scientists looking to maintain longevity of the effect being studied on the cell. During stable transfection, once the DNA has been expressed by the cell, the target gene has inserted itself into the cellular genome and therefore replicated with the cell's genomic DNA. This is ideal for large scale experiments or mass production for a particular recombinant protein or vaccine production.

The other type of expression is transient transfection which can only maintain expression for short periods of time since the foreign DNA is only introduced to the eukaryotic cell itself but is not integrated into the cellular genome. This method is used for small-scale production and testing short-lived expression antibody production, recombinant cassettes with plasmid DNA, and chemical delivery systems for nucleic acids [88]. Transient expression is the preferred method for achieving quick and efficient transfection in a short amount of time and generating high throughput of messenger RNA (mRNA) to use for evaluation of the results. It has been recently investigated whether a selective marker is needed in order to monitor the expression of genes [89]. The expression of plasmid DNA in this transient experiment may be sufficiently monitored without the use of a selective marker, but instead by GFP expression and fluorescent microscopy [90]. Another crucial component to the validity of the experiment is having accurate controls tailored to what the scientist is investigating. The problem that occurs when dealing with FMDV is the lack of available resources used specifically for testing against the immunogenic epitopes within the vaccine and determining true controls for the experiment. Louisiana State University also has strict regulations and precautions set in place when dealing with infection pathogens as well as meeting certain requirements by the distributor ultimately halting efforts towards that approach.

1.10. Justification and Hypothesis

The overall goal of this project was to design a DNA vaccine capable of cross- protection against FMDV serotype O infection. Using bioinformatic technology and *in-silico* analysis, immunodominant proteins of FMDV serotype O were used for the construction of a multi-epitope DNA vaccine. The hypothesis is the recombinant DNA vaccine for FMDV serotype O will be transcribed in eukaryotic cells and detect significant amounts of protein expression.

Current biosecurity measures for FMDV in developing countries are not enough to maintain the reduction of the disease pathogen throughout livestock. With its highly infectious nature, new and novel vaccine approaches are needed to prevent this disease.

This design utilized an immunodominant epitope, containing most of the P1 region, alongside 2A and 3C protease, proven in the past to elicit a cellular immune response against specific serotypes. The IL-18, a strong genetic adjuvant, included in the vaccine design to combat possible poor transfection rates. Enzyme-linked immunoassay (ELISA) kits for detection are available but lack specificity. Vaccines against strictly structural proteins allow for differentiation, as antibodies in an infected animal can be found against nonstructural proteins. After conducting a preliminary literary search for the selection of FMDV epitope candidates, the importance of structural proteins VP1, 2, and 3 has been greatly evidenced to play a critical role for capsid stability, maturation, virus binding and antigenicity. An optimized and stable Porcine IL-18 based immunoglobulin (Ig) G as a serological logical tool for the FMD vaccine is a potential benefit for future testing cell lysate production.

The aim of this vaccine is also to be cost-effective, which is critical given that the nature of the pathogen is found in economically developing regions. The vaccine component was cloned into the backbone vector pBSX, previously used in Dr. Cooper's lab. Moreover, this vaccine design and methodology could lead to the implementation of a new and safer approach to address FMD.

The aims of this study are as followed:

1. Design and construct a DNA vaccine with immunogenic epitopes for FMDV serotype.
2. Optimize ELISA positive and negative controls for future FMD DNA vaccine testing.
3. Determine if DNA vaccine will be transcribed in HEK cells.

4. Determine if DNA vaccine will be transcribed in CHO cells.
4. Determine if protein expression of DNA vaccine will occur
5. Determine optimal transfection reagents and cell line for future FMDV DNA vaccine testing.

Chapter 2. Materials and Methods

2.1. Vaccine Construction

2.1.1. Antigen and Epitope Selection

First, estimated locations of the antigenic proteins were identified within the 2018
Zambian Type-O strain². The strain of choice was located at the National Center for
Biotechnology Information (NCBI) under the GenBank number AMN16576². The genome that
we selected was fully sequenced but was not fully annotated so we could not readily determine
the locations of the desired proteins. In order to do this, we compared our amino acid sequence to
other fully annotated sequences of other strains of Type O to identify sequence similarities using
NCBI's Protein Blast program [84]. Blasts were performed against the following fully annotated
GenBank entries of available and fully annotated FMDV polyprotein sequences: AYQ95738.1,
AOG20774.1, AZS18886.1, and AHZ45958.1 [1,2]. The former two were FMDV type-O strains
and had identity values of 97%. The latter two were FMDV type-A strains and had identity
values of 92%. The four annotated strains indicated the following amino acid (aa) sequence
similarities within proteome sequence: VP1= 725- 937 aa, VP2= 287- 504 aa, VP3= 505- 724 aa,
VP4= 202- 286 aa, 2A=938- 953 aa, 3C-protease= 1650- 1862 aa. Since the identity values were
above 90% for all the blasts, these amino acid sequences were determined to be the approximate
locations of the VP1, VP2, VP3, VP4, 2A, and 3C protease genes within AMN16576.1.

The Immune Epitope Database and Analysis Resource (IEDB) website was used to
identify immunogenic epitopes within the proteins selected [85]. Protein sequences were
analyzed using the T cell epitope prediction software for predictions of major histocompatibility

² The time of epitope selection was in 2019 and the polyprotein of Foot-and-mouth-disease virus O/ZAM14/2010 strain was the most recent fully annotated sequence available.

complex II (MHC-II) binding. However, this software does not offer bovine as an organism for analysis, therefore, to possibly circumvent this issue protein sequences were analyzed against all available species and a random selection of alleles within them. Ultimately, the analysis conducted included 3 mouse alleles and 9 human alleles. Predictions were produced for three mouse H-2-1 alleles (H2-IAb, H2-IAd, H2-IEd), three human HLA-DP alleles (HLA-DPA1*01/DPB1*04:01, HLA-DPA1*01:03/DPB1*01:01, HLA-DPA1*01:03/DPB1*02:01), three human HLA-DQ alleles (HLA-DQA1*01:01/DQB1*02:01, HLA-DQA1*01:01/DQB1*02:02, HLA-DQA1*01:01/DQB1*02:03), and three human HLA-DR alleles (HLA-DRB1*01:01, HLA-DRB1*01:02, HLA-DRB1*01:03). According to IEDB's algorithm, the lower the percentile number, the higher the affinity between the antibody and the epitope, and therefore, the more immunogenic potential of the epitope (13, 14). Peptide sequences with percentile rankings of under 5% were considered to have a high affinity between epitopes and antibodies and therefore be immunogenic. Portions of the peptide sequences that had high affinity rankings with the most alleles were selected as the epitopes for this vaccine (see Table 2.1 and Table 2.2).

Table 2.1. Final amino acid sequences selected for each antigenic epitope of vaccine.

Protein Name	VP1	VP2	VP3	3C protease
Protein	TATVENYGGTTQV	MRNGWDVEV	FEGDVPYVTTKTE	PRHLFAEKYDRIML
Sequence	QRRQHTDVSFILDR	TAVGNQFNGG	SDRVLAQFDLSLA	DGRAMTDSYRVFE
	FVKVTPQDQINVLD	CLLVAMVPEL	AKHMSNTFLAGL	FEIKVKGQDMLSDA
	LMQIPAHTLVGALL	CSIQKRELYQL	AQYYTQYSGTINL	ALMVLHRGNRVRDI
	RASTYYFADLELA	TLFPHQFINPR	HFMFTGPTDAKAR	TKHF
	VKHEGNLTWVPNG	TNMTAHITVP	YMIAYAPPGMEPP	
	APEAALDNTT	FVGVNRY	KTPETA	

Source: IEDB Analysis Resource [85]

Table 2.2. MHC-II binding predictions within the selected epitope region

Species		VP1	VP2	VP3	3C protease
	Mouse, H-1-2	✓ ✓	✓	✓ ✓	✓
	Human, HLA-DP	✓ ✓ ✓	✓ ✓ ✓	✓ ✓	✓ ✓
	Human, HLA-DQ	✓ ✓ ✓	✓ ✓	✓ ✓ ✓	✓ ✓ ✓
	Human, HLA-DR	✓ ✓ ✓	✓	✓ ✓	✓ ✓

Notes: The check marks indicate the number of alleles that had <5% MHC-II binding predictions within the selected epitope region. VP4 produced very few immunogenic predictions and was removed from the vaccine design to reduce the vector size. The peptide sequences chosen were then entered into MS Excel ® to organize the order they appear in the genome and highlight desired regions

Source: IEDB Analysis Resource [85]

2.1.2. Vaccine Components and Placement

The SV40 NLS was placed 5' to the CMV Promoter within the pCPP Backbone Vector was cloned from previously designed and tested vaccines within Dr. Cooper's laboratory and incorporated into the final vaccine sequence. The bovine MIP-1 α signal sequence utilized in the vaccine design was obtained from the UniProt website under entry number Q8SQA6 and entry name CCL3_BOVIN. To best maintain protein folding when generating T cell epitope predictions with IEDB, epitopes were placed in the order they would occur naturally in, VP2, VP3, VP1, 2A, followed by 3C, each separated by an FRS sequence. Epitopes were preceded by the MIP-1 α signal sequence and followed by the genetic adjuvant, swine Interleukin-18 gene. Lastly, after the adjuvant and signal sequence was designed, BGH polyA was chosen as the polyadenylation signal sequence attached at the 3' end.

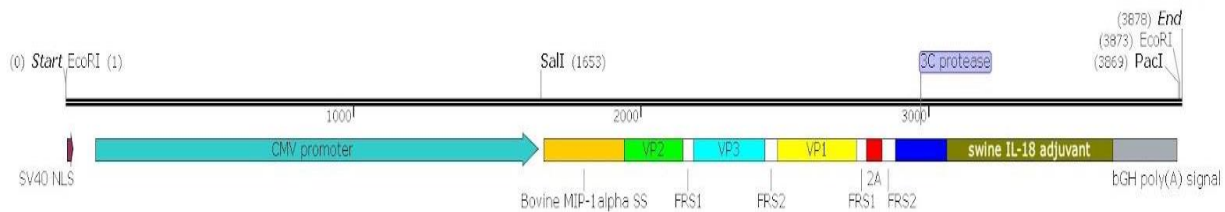


Figure 2.1. Linear representation of pFMDV1 DNA vector components starting with nuclear localization sequence, SV40, CMV promoter attached to epitope selections intercalated with FRS, preceded by a bovine MIP-1 α signal sequence and followed by a swine IL-18 genetic adjuvant and finally bGH specific polyA signal sequence. (Made with GeneSnap)

Once the theoretical vaccine sequence was constructed, the amino acid sequence was codon optimized by the Integrated DNA Technologies' (IDT) codon optimization tool. All the codons were optimized for *Bos taurus*.

2.1.3. Restriction Enzyme Sites

To minimize costs, the pFMDV1 vaccine was designed as a cassette, or insert, for cloning into the pCPP backbone vector using unique restriction enzyme sites. The pFMDV1 coding sequence was synthesized by IDT in the pUCIDT-ampicillin vector flanked by SalI restriction enzyme at the 5' end and poly A tail at the 3' end. The vaccine also included uniquely placed restriction enzyme sites, PacI, BglII, and EheI with extra base pairs in between each cutting site to allow enzymes to bind efficiently. The FMDV vaccine was cloned into the backbone vector, CMV pBS puro (pCPP) backbone vector, previously sequence verified. Restriction enzyme sites of SalI and PacI were added to pCPP beforehand such that the vaccine open reading frame would be cloned in the correct orientation with the CMV promoter in CPP.

2.1.4. Determination of Epitope Preservation

Prior to ordering FMD vaccine, the amino acid sequence was analyzed in IEDB's T-cell prediction software for MHC-II binding predictions. The greater ability for MHC-II to bind with the epitope necessary for activating CD4⁺ cells and act as helper function while also substantially increasing the cytokine production by Th1 cells. This analysis was performed using the same parameters used for epitope selection against the same 12 common alleles. All the chosen epitopes maintained their binding predictions. This indicated that neither the codon optimization nor the epitope size and arrangement of vaccine components altered the epitopes' affinity to bind with the antibodies.

2.1.5. Testing Complexity

The final pFMDV1 vector was analyzed on the Integrated DNA Technologies (IDT) website for complexity of DNA sequence synthesis. The complexity score from IDT was 29.6. This score is considered moderate to high, making the vaccine "tentatively" possible to synthesize. IDT detected 3 hairpins, several regions containing repeating sequences, and several

guanine-cytosine rich regions, which could make vaccine construction difficult. It is an important step especially with a vaccine of higher complexity and ensuring cloning of the vaccine components done correctly.

2.2. Transformation and Cloning

The pFMDV1 DNA was ordered from IDT in the pUCIDT-Ampicillin vector (pFMDV1) flanked by SalI at the 5' end and poly A tail at the 3' end attached to uniquely placed restriction enzyme cutting sites, PacI, KpnI, and EheI. Extra base pairs were added in-between each cutting site to allow restriction enzymes enough bps to sufficiently excise the correct bands. The pFMDV1 was transformed using *dam⁻/dcm⁻* competent *Escherichia coli* cells (New England BioLabs, Cat #C2925H) according to manufacturer's protocol then spread on 1/2 Super Broth ampicillin (SB/amp) agar plates and incubated at 37°C overnight. Resulting colonies were picked with a sterile toothpick inoculated into ml of 1/2 SB AMP broth, incubated overnight in a shaking incubator at 37°C and 100 rpm. Plasmid DNA was harvested by a mini-preps procedure from the overnight broth mixture following the ZymoPure's Classic Mini-prep Kit followed by archiving 50 ul of the mini-prep on a 1/2 SB AMP Plate. Once plasmid size was confirmed, colonies from archive plate of pFMDV1 minipreps were scaled up to a midiprep to prepare enough DNA concentration for excision and ligation into the backbone vector, pBlue CMV Puro (pCPP). The newly made pFMDV1 midiprep was quantitated using the NanoDrop at a concentration of ul/ml.

A previously sequenced verified pCPP midiprep stock stored at -20 C was thawed and transformed using *dam⁻/dcm⁻* competent *Escherichia coli* cells following the same cloning procedure as pFMDV1 DNA except only midipreps were performed on pCPP. The pCPP was quantitated using the Nanodrop under the same conditions as pFMDV1 midipreps. The pCPP midiprep was then double digested using EheI and SalI restriction primers to open the vector of

6076 bp at the specific cutting sites and prepare for ligation with pFMDV1. The newly digested pCPP band was clean and concentrated following ZymoPure's Clean and Concentrate instructions then electrophoresed on a 1% ethidium bromide gel to make sure the band was the correct size.

The original pFMDV1 vector was 5032 bp was digested with restriction enzyme cutting sites *EheI* (2755b bp) and *SalI* (491) located at opposite ends with the band containing the pFMDV1 vaccine a total of 2264 bps and the amp (+) vector that the pFMDV1 vaccine was delivered in now a band length of 1839 bp. Due to the similar size in band length band with only a 300 bp difference, it would be hard to tell which band is correctly excised for ligation with pCPP. A third restriction enzyme site, *PdmI* (4644bp) was used to cut the amp (+) band making two smaller DNA pieces now leaving the FMDV1 band now easily detected when analyzed on a SyberSafe Gel. A 1% SyberSafe Gel was conducted on pFMDV1 followed by extracting the band from the gel and purifying using Zymo's DNA Recovery Kit per manufacturer's instructions to prepare for ligation with pCPP clean and concentrated digest.

The digested pCPP (6076) allows ligation of the pFMDV1 (2028 bp) between the CMV and the Poly A of the vector through ligation. Ligation protocol was followed using Instant Sticky End Master Mix (New England Biolabs, Cat # M0370) then transformed in competent *E. coli* as described previously. Colonies were picked from transformation archive plates and scaled up for midipreps. The newly ligated pFMDV1/CPP vector was analyzed using restriction enzyme, *BglIII*, in a test digest to determine if pFMDV1 successfully cloned into pCPP. In SnapGene, *BglIII* cutting site was strategically placed in FMD1 vector design because it is not present in CMV Puro. Midipreps containing both pFMDV1 and CMV Puro were also digested using *PacI* and *SalI* to ensure the vector is present and not lost upon digestion. The midiprep

products were sent to Gene Probes and Expression Systems Laboratory/LSU BioMMED (LSU Gene Laboratory) for sequence verification before attaching the nuclear localization sequence (NLS). Phosphorylated primers serving as the NLS gBlock at only 152 bps in length was ordered to be directly ligated with pFMDV1/CPP as seen in Table 2.3.

Table 2.3. Oligonucleotide DNA Specification

Primers	5'-/Phos/ sequence-3'
FMD NLS bottom 2 phos	GGG GGA GCC AAA CTT TTC TTT TTT TTT TTG GCG CGA GAC AAT TAA CCG
FMD NLS top 2 phos	GGGGGAGCCAAACTTTTCTTTTTTTTTTTGGCGCGAGACAATTAACCGC

Notes: Specific NLS gblock ordered as phosphorylated oligonucleotides that act as primers to be ligated with pFMDV1/CPP

Source: IDT Laboratories

Plasmid containing pFMDV1/CPP (8310 bp) was digested using restriction enzymes, NotI (6033 bp) and SmaI (6000 bp) that have unique cutting sites located close to each other between the CMV and the very beginning of the 5' end. The newly digested band is ligated with NLS following the NEB ligation protocol to create a new plasmid, mFMDV1/CPP/NLS which was transformed into *E. coli* and scaled up for midipreps. The pFMDV1/CPP/NLS midiprep was quantitated at a concentration of 3066.3 ng/ul and 260/280 absorbance. Due to the small band size of NLS, confirmation via test digest was not used. Instead, a PCR amplifying the NLS region of vector using custom oligonucleotide primers ordered from IDT, NLS Primer 1 and NLS CMV primer 2 as seen in table 4. PCR thermocycler conditions were followed according to the manufacturer's protocol with an annealing temperature of 52 C. The pFMDV1/CPP/NLS midipreps were then submitted to LSU Gene Laboratory for sequence verification. To reduce the size of the vector and because there was no selective antibiotic used in cell culture, the sequence verified 3-1 Puro gene was excised from pFMDV1/CPP/NLS. Restriction enzyme cutting sites located at ClaI (1066 bp) and NarI (2070 bp) were cut excising the 1000 bp puro gene leaving the

newly digested pFMDV1/NLS at 7348 bp. The band was then ligated with itself and transformed to grow up for midipreps. Custom DNA oligonucleotides ordered from IDT were used to assess specific primer focus regions. Target regions include 370 bp to 570 bp where the CPP is located and between 1835 to 2035 bp where only FMDV1 and NLS is found. To check that the CPP is present, PuroCheck F and CMV R1 were used. For confirmation that pFMDV1 and NLS DNA is present, Mia FMD F and Mia FMD R were created. Midiprep products were sent to LSU Gene Laboratories for final sequence verification before use in *in vitro* testing.

Table 2.4. Primers used for Sequence Verification and PCR amplification.

Primer Name:	Primer Sequence 5' to 3'	Annealing Temp
Puro Check Fwd	CCATGGGTCTTTTCTGCAGTCACCGTCACCGTCTCG	67 °C
CMV Rev1	CGAGACGGTGACTGACTGCAGAAAAGACCCATGG	67 °C
FMD Fwd 1 (mar22)	ATTTCGCGGATCTTGAACCTGGCAG	63 °C
FMD Rev 1 (mar22)	ACTCTGGACGTGTCCAGCCAAC	63 °C
Mia F FMD	TGGAACAACACTCAACCCTATC	52 °C
Mia R FMD	GCCAGGATTGGGAAGACAATAG	52 °C
NLS Primer 1	CGGTAAATTGTCTCGCGCCAAAAAA	56 °C
NLS CMV primer 2	AAGTCCCGTTGATTTTGGTGCC	56 °C
Gapdh F	GAAAGCTGTGCTGATT	57.1 °C
Gapdh R	TACTTGGCAGGTTTCTCCAG	57.1 °C
GFP Fwd	GGCCTGCCC GCCATGGAGATC	63 °C
GFP Rev	ACCGGCATCTGCATCCGGGG	63 °C

Source: IDT Laboratories

2.3. Cells and Transfection

The pFMDV1/NLS vaccine was transfected *in-vitro* using HEK293 and CHO-K1 cells (ATCC) complexed with transfection reagents, as described in Table 5. Media, cell lysates, and mRNA were collected from transfected cells as well as non-transfected cells. Green fluorescent protein (GFP) was used as a reporter gene under the same conditions in both cell lines simultaneously to visually monitor transfection efficiency.

Prior to beginning cell culture, freeze-backs for both sequence verified midipreps, pFMDV1/NLS and pGFP2, were thawed, transformed and cloned for midipreps, then quantitated using the NanoDrop to assess the amount of DNA needed for transfection protocol. The pGFP2 plasmid was previously constructed and transfected using SHC003BSD-Del GFPD vectors (Addgene, #133302) cloned into plasmids then labeled as pGFP2.

Cells were viewed under microscope 24 hours post-transfection as determined from previous GFP experimentation.

Cell Culture was performed under sterile conditions in a LabGard Class II, Type A2 Biosafety Cabinet (Nuair) and all instruments were sterilized prior either by autoclaving or delivered from manufacturer as sterile. Prior to obtaining cells, cell culture media was prepared (K. McDonough, personal communication): 10% or 20 mLs of heat inactivated Fetal Bovine Serum (FBS) (SAFC Biosciences Inc, Cat # 54616C) was added to 178 ml of F-12 (1X) Nutrient Mix (Ham) [+] L-glutamine (Gibco, Cat # 21700-075) along with 2 mLs of GlutaMax (Gibco, Cat # 12551032). A stock culture CHO K1 Cells (ATCC, Cat # PTA-3765) was recovered from a liquid nitrogen freezer and propagated in 20 mLs of cell culture media that was pipetted into a 75 cm² cell culture canted neck flask (Corning), housed in a Sanyo MCO-18AIC (UV) CO₂ Incubator (Marshall Scientific, Hampton, WV, USA) atmosphere of 5% CO₂ at 37°C. CHEK 293 cells were treated using the same conditions as CHO-K1 throughout the entire experiment except

being fed a nutrient mix using 20 mLs of Dulbecco's Modified Eagle Medium (DMEM) (Gibco, Cat # 30-2002) supplemented with 10 % of FBS. The parent flask was incubated for 24 hours to reach 80% confluency. To split the cells, each flask was washed with 10 mLs of Dulbecco's phosphate buffered saline (DPBS) supplemented with calcium and magnesium (Gibco, Cat # 14-040-133).

The adherent cells were then detached by trypsinization using 2 mLs of TrypLE Express (GIBCO, Cat # 12605-010). The detached cells in the 2 mLs of TrypLE Express was evenly pipetted and passed into two new flasks. The parent flask and the two new flasks were then diluted in 15 mLs of respective cell culture media.

This step was repeated until enough flasks were passaged to support experimental groups. All flasks were randomly assigned to groups 1 through 7 with three flasks belonging to each group and an extra three supplementary flasks as a precautionary measure for a total of 24 flasks. Calculations for volumes of transfection reagents were based on scaling up the growth area from a well of a 6-well plate to the growth area of a T75 flask as suggested by Corning Flasks for ThermoFisher. The optimum transfection size/density is based on 6-well culture vessel with a growth area of 9.6 cm²/well and total volume per well/cm² of 125 ul. A Corning T-75 U shaped Canted Neck Cell Culture Flask with a Vent Cap is 75 cm² for surface area and total volume per well/cm² of 0.1 mLs. There are 7.81 total wells equivalent to the vessel size for a T75 flask. Calculations used 7.81 as the multiplication factor times the number of flasks needed for determining the transfection reagent complexes.

Groups 1 through 3 were used as controls throughout the entire experiment. Group 1 was used as a negative control with no transfection reagent or complexed DNA. Group 2 and 3 were used as transfection controls with Lipofectamine 3000 (Invitrogen Cat. #L3000001) or

JetOPTIMUS DNA transfection reagent system (VWR, Cat #76299-632) but no complexed DNA. Group 4 was transfected with Lipofectamine 3000 reagent and complexed with pFMDV1/NLS DNA. Group 5 was transfected with Jet Optimus and complexed with pFMDV1/NLS DNA. Group 6 and 7 followed the same conditions for transfection reagent as group 4 and 5 respectively but was complexed pGFP2 transfected DNA. The layout of the transfection groups for the experiment can be seen in Table 5. Cells were seeded 24 hours prior to transfection in associated growth media at a density of 5.4×10^4 viable cells/cm².

	Transfection Reagent :	Complexed DNA :
Group 1	No transfection reagent	Non-transfected DNA
Group 2	Lipofectamine 3000	Non-transfected DNA
Group 3	Jet-Optimums	Non-transfected DNA
Group 4	Lipofectamine 3000	pFMDV1/NLS transfected DNA
Group 5	Jet-Optimums	pFMDV1/NLS transfected DNA
Group 6	Lipofectamine 3000	pGFP2 transfected DNA
Group 7	Jet-Optimums	pGFP2 transfected DNA

Figure 2.2. Transfection groups for both CHO-K1 cell line experiment and the HEK-293 cell line experiment. (Made with Biorender)

Notes: Each group represents three reactions using T75 cm² flasks with a total of 21 flasks for each treatment. Groups are further categorized based on transfection reagent. Group 1 serves as the negative control for the experiments with non-transfected DNA without any reagent added. Group 2 and 3 serve as positive control groups with a transfection reagent present but non-transfected DNA. Group 4 and 5 test transfection reagents for complexed DNA containing pFMDV1/NLS. Group 6 and 7 test the two transfection reagents against the reporter gene pGFP2 to monitor transfection within the cells.

2.4. Optimized Serological Testing

Interleukin 18 (IL-8) (AA 36-192) protein (I7 tag, His tag) was used as the protein. Purified IgG1Mouse Anti-Pig Interleukin-18 non-conjugated antibody (antibodies-online Inc., Cat. # ABIN6236565, Batch # 1603) was used as the positive primary monoclonal antibody. Mouse IgG Negative Control (Bio-Rad MCA928, Batch # 151536) was used as the negative primary monoclonal antibody. Goat anti mouse IgG: HRP (RAT AD) (Bio-Rad STAR77, Batch # 1801) was used as the secondary antibody.

The IL-18 protein (1 x 50 ug) was reconstituted using 500ul Ultrapure DNase/RNase-Free Distilled Water (ThermoFisher Scientific, Cat. #10977015) and aliquots of the entire reconstituted protein were pipetted into 1.5 ml cryopreservation storage tubes (Nalge-Bunch International, Cat. # 05538718) then stored in -80 C Panasonic Freezer. On the day of preparing the ELISA plate, one of the IL-18 protein aliquots was thawed, 62.5 ul pipetted into a 1.5 mL Safe-Lock Tube (Eppendorf, Cat. #0030119380). The initial protein concentration was diluted by adding 4937.5 ul of DPBS (ThermoFisher Scientific, Cat. # 11965084) to prepare a starting serial dilution of 1.25 ng per well. 2.5 mL of the first tube was then added to a second tube with 2.5 mL of DPBS to achieve a working dilution of 0.625 ng per well, then repeated one more time to obtain one final working dilution of 0.312 ng per well. Duplicates of each serial dilution of IL-18 protein were pipetted (100 uL per well) to their respective wells assigned to on an uncoated 96 well ELISA plate (Biolegend Nunc MaxiSorp, Cat. #23501) as seen in Figure 2.2.

ELISA PLATE LAYOUT

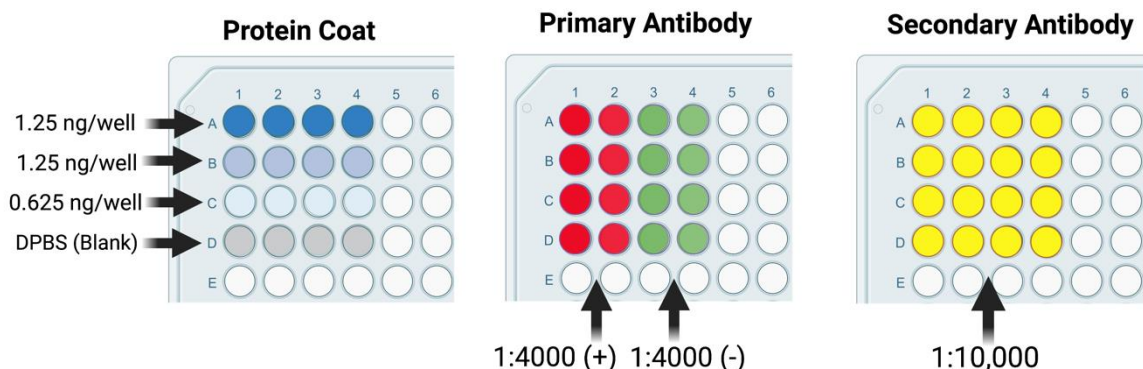


Figure 2.3. Layout for ELISA Plate. (Made with Biorender).

Notes: A 96-well uncoated ELISA Plate (100 μ l per well) for each step including the initial protein coat replicated in groups of four seen in blue. For primary antibody, the primary positive (+) antibody replicated in duplicates seen in red and the negative (-) primary antibody replicated in duplicates seen in green. The secondary antibody was replicated across the entire grid as seen in yellow.

The entire ELISA plate was coated with 100 μ l of 0.5 M in house bicarbonate buffer solution, pH 9.6 (coating buffer). The plate was incubated at 4 C overnight to ensure antigens were immobilized on the well surface. After this incubation, the residual coating solution is dumped off by flicking the plate over a sink then firmly patting the plate face down on a clean paper towel. 200 μ l of a 1% BSA solution was added to each well to block remaining protein binding sites. Plate was then incubated for two hours at room temperature on a titer plate shaker (Lab-Line Instruments/ThermoFisher Scientific, Cat. # 4625Q). Residual BSA solution was then dumped off again and washed using a 1X PBS wash buffer solution. Primary antibodies were diluted using in house 1% BSA (found in appendix: Protocols: 1% BSA) in 10 mL conical tubes by pipetting 1 μ l of stock into 4,000 μ l of 1% BSA. Duplicated of both primary antibodies were pipetted into their designated well as seen in Figure 2.2. The plate was then incubated again for 2 hours at room temperature on the titer plate shaker. The residual dumping and wash step using 1X PBS was repeated. In a 1.5 mL tube, 2 μ l of the conjugated secondary antibody was diluted in

2 ul of 1% BSA to create a working dilution. 1 ul of that dilution was added to 5,000 ul of 1% BSA in a 10 mL conical tube to reach a final dilution of 1:10,000. The secondary antibody in blocking solution were then pipetted into each well across the entire plate. Finally, the plate was incubated on the titer plate shaker for two hours followed by dumping and plate wash for final detection reagents. 100 ul of Tetramethylbenzidine (TMB) single-component substrate solution (Solarbio, Cat. #34028) was added to plates. The plate was monitored over a 30-minute period on the shaker for signs of color change indicating the reaction is taking place. Once the desired color has been reached, in this case blue, or 30 minutes had elapsed, 100 ul of 2 M sulfuric acid solution was added to stop the reaction turning solution of each well yellow. The ELISA plate was read by the Benchmark PlusTM microplate spectrometer (Bio-Rad Laboratories, Model 680) through 9.1 microplate manager software. ELISA detection of any conjugated protein signal and binding levels were measured at an optical density of 450 nm.

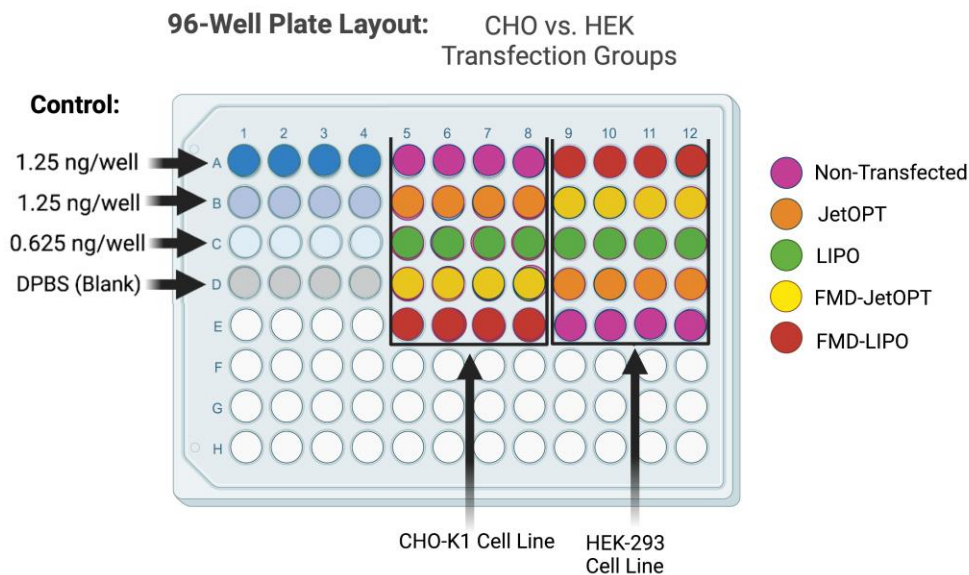


Figure 2.4. Layout for ELISA. (Made with Biorender).

Notes: 96-well uncoated Plate (100 ul per well) for comparing protein expression using the standard coat from Figure 2.2. The initial protein coat for both cell lines from the five transfection groups were replicated in groups of four and can be identified by the color key on the right. Wells were filled with 100 ul pipetted directly from cell lysate aliquots.

The standard curve to be used for protein detection was determined using GraphPad Prism 8 software, the Pearson correlation coefficient (r) with P-value (0.05) was used to interpret the protein (ng) absorbance readings of different primary and secondary concentrations to establish controls for ELISA testing. The coefficient was used to measure the strength and direction of a linear relationship between different concentrations. The (r)values were interpreted as looking for any values closest to -1 for a strong negative relationship with no correlation, and values closest to 1 for a strong positive relationship.

The ELISA output from the Benchmark Plus TM microplate spectrometer was computed into GraphPad using the standard curve as a base line for protein detection using a two-tailed p value summary looking for any significance for protein expression.

Chapter 3. Results

3.1. Verification of Vaccine Size and Placement

Verification of DNA plasmid constructs were confirmed using diagnostic restriction digests and DNA sequencing. Before sequence verification, gel electrophoresis was used to validate that the plasmid size, digested DNA fragment size, and PCR product size. Plasmids pFMDV1 and pCPP were successfully transformed. pFMDV1 minipreps confirm the size of 5032 bps via 1% Gel electrophoresis size and bright bands and indicated a decent amount of DNA concentration to work with as seen in Figure 3.2. pFMDV1 were successfully grown up to midipreps. The concentration for the pFMDV1 midiprep was 955.65 ng/ul. The pCPP midiprep concentration was determined to be at 166 ng/ul, which was enough to warrant moving forward with digestion and ligation. The newly clean and concentrated pCPP double digest matched the correct expected size of 6070 bps from SnapGene confirmed by 1 % Gel electrophoresis in Figure 3.1. The newly cut pFMDV1 band after triple digest (2264 bp) showed successful digestion as seen in Figures 3.3 and 3.4. pFMDV1/CPP was successfully ligated and transformed as confirmed via 1% Gel electrophoresis as seen in Figure 3.5 and sequenced verified by Gene Laboratories. NLS was successfully ligated with pFMDV1/CPP as seen by both gel electrophoresis, confirming that pFMDV1/CPP vector was lost upon digestion (Figure 3.6) and NLS was present by PCR (Figure 3.7). pFMDV1/CPP/NLS was successfully transformed and grew up for midipreps. pFMDV1/CPP/NLS midiprep was sequence verified by Gene Laboratories. The puro gene was successfully excised after double digestion confirmed via PCR as seen in Figure 3.8. The pFMDV1/NLS vaccine was successfully transformed and grew up for midipreps with a final concentration quantitated at 457.6 ng/ul with an absorbance of 260/280 at

(a) Gel electrophoresis image showing four lanes. Lane 1: 1 Kb Ladder. Lane 2: pCPP midprep. Lane 3: pCPP double digest Ehel/Sall. Lane 4: pCPP double digest (C+G) Ehel/Sall. Molecular weight markers are indicated on the left: 10000 bp, 5000 bp, and 1000 bp. A red box in lane 4 highlights a band at approximately 6076 bp.

(b) Plasmid map of pBlue Puro CMV (CPP). The map shows a circular plasmid with the following features: AmpR (Ampicillin resistance), MCS (Multiple Cloning Site), lacZα (lacZ alpha), CMV Intron, CMV promoter, and a SalI/EcoRI site. The map also indicates the location of the SalI and EhoI restriction sites.

a.)

Supercoiled Ladder
pFMDV1 Midiprep 1
pFMDV1 Midiprep 2

2280 bp

b.)

pUC IDT FMDV1 Linear Vaccine

EheI SalI

lacZ α

VP2

VP3

VP1

FUS2

2A

VP4

41

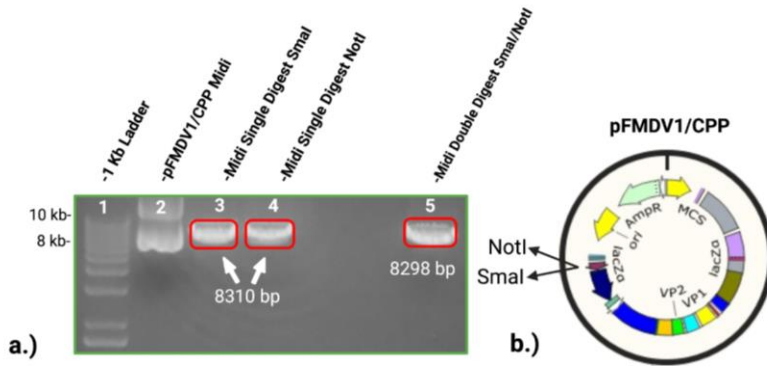


Figure 3.5. Gel Confirmation of pFMDV1/CPP showing correct sizes. On the left (a.) is a 1% small ethidium bromide gel. In well 1 is 5 ul of 1kb ladder followed by 5 ul pFMDV1/CPP midprep acting as control in well 2. Well 3 is 5 ul pFMDV1/CPP midprep after digestion with SmaI and a total vector size of 8310 bp. In well 4 is 5 ul pFMDV1/CPP midprep after digestion with NotI. In well 5 is 5 ul pFMDV1 midprep after double digestion with both SmaI and NotI with a vector size of 8298 bp. On the right (b.) is the pFMDV1/CPP vector map where these restriction sites are located.

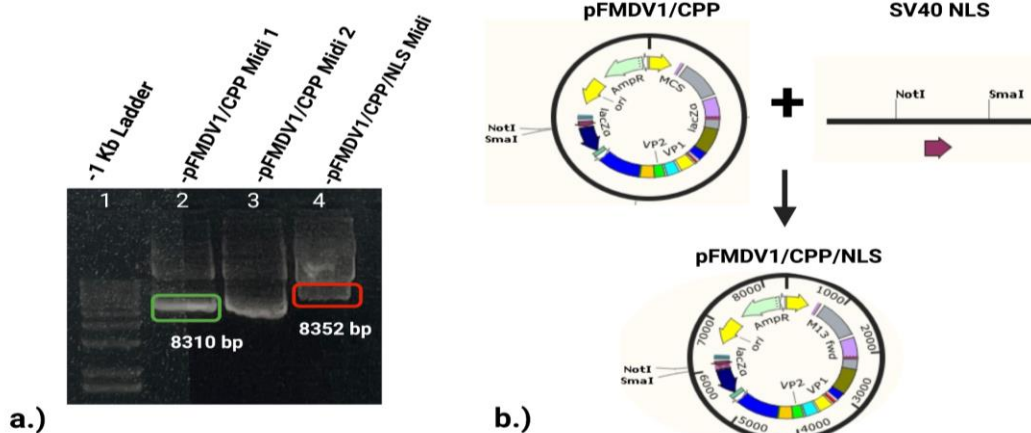


Figure 3.6. Gel Confirmation of pFMDV1/CPP/NLS showing correct sizes. On the left (a.) is a small ethidium bromide gel with a 1 Kb ladder in well 1. In well 2 and 3 is 5 ul pFMDV1/CPP midprep 1 and 2 and 5 ul of pFMDV1/CPP/NLS in well 4. On the right (b.) is the vector map of pFMDV1/CPP at 8310 bps and SV40 NLS (phosphorylated linker) which should be around 152 bps. The arrow is pointing to the newly formed plasmid, pFMDV1/CPP/NLS which should only differ about at 152 bps.

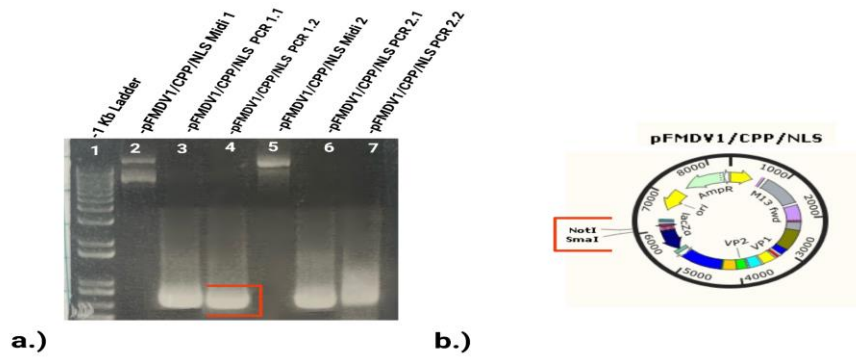


Figure 3.7. Gel Confirmation of pFMDV1/CPP/NLS PCR and showing correct sizes. On the left is (a.) is a small ethidium bromide gel with a 1 Kb ladder in well 1. In well 2 and well 5 is pFMDV1/CPP/NLS Midiprep. 1 and 2 respectively. In well 3 and 4 and 6 and 7 are PCRs Confirmation of pFMDV1/CPP/ NLS on a 1 % Ethidium Bromide Gel. PCR samples using pFMDV1/CPP/NLS Midiprep (at a concentration of 3066.3 ng/ul; 260/280 absorbance of 1.84) and pFMDV1/NLS (457.164 ng/ul; 260/280: 1.91) at 1:10 working dilution using [10x] TE Buffer. Mia FMD F and Mia FMD R primers were also diluted to a 1:10 working dilution using dH₂O. Annealing temp is set at 52. On the right (b.) is the expected outcome for extension time and bp length of PCR amplified DNA for both pFMDV1/NLS matched sequencing verification as well as evidence that transcription took place.

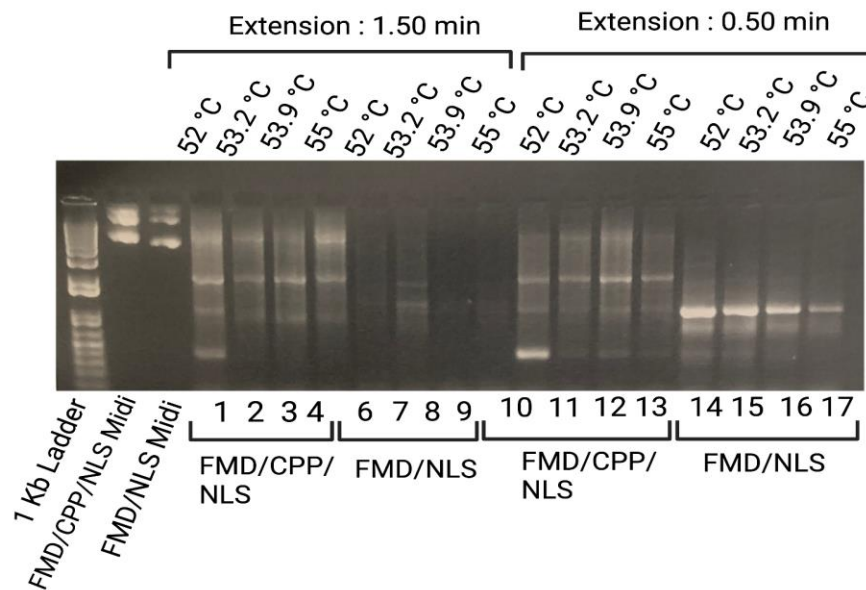


Figure 3.8. Gel Confirmation of pFMDV1/CPP/ NLS showing correct sizes for a PCR on 1 % Ethidium Bromide Gel. PCR samples using pFMDV1/CPP/NLS midiprep (at a concentration of 3066.3 ng/ul; 260/280 absorbance of 1.84) and pFMDV1/NLS (457.164 ng/ul; 260/280: 1.91) at 1:10 working dilution using [10x] TE Buffer. Mia FMD F and Mia FMD R primers were also diluted to a 1:10 working dilution using dH₂O. Samples were divided into two groups based on extension time of Thermocycler. Group One, which contained subgroups A and B, were set for 1 minute and 30 seconds at 68°C. Group 2 containing subgroups C and D were set for 50 seconds at 68°C. Subgroups A and C were DNA samples containing puro while subgroups B and D were DNA samples without puro.

3.2. *In Vitro* Results

Midipreps for both pFMDV1 and GFP2 plasmids had a similar concentration of 1110 ng/ul with the same absorbance ratio of 260/280 at 1.853. RT-PCR in Figure 3.9 matched the desired outcome with the transfected mRNA for the vaccine specific primers as well as a band appearing for the HK primers confirming that pFMDV1/NLS was in fact expressed in CHO-K1 cells as seen in Figure 3.9 lighting up green. The non-transfected mRNA did not react with the experimental primers but was in fact brighter with the HK primers showcasing that non-transfected CHO-K1 mRNA could be used as a true negative control as confirmed by RT-PCR in Figure 3.9 as well as fluorescence images in 3.10.

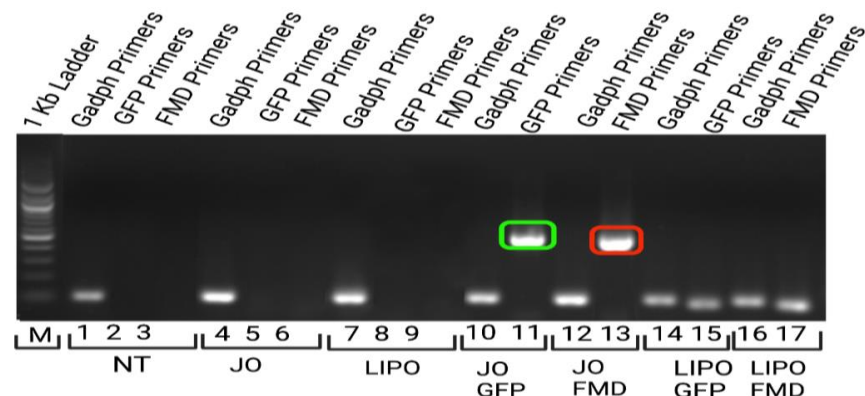


Figure 3.9. Confirmation of cDNA expression for both pGFP2 and pFMDV1/NLS in CHO-K1 cells. In well 1 is Kb ladder. Wells 1,4,7,10, 12, 14, and 16 are for the confirmation that CHO-K1 cells are in fact present. A band should be present across the entire gel. Well 11 in the green box is the band for confirmation for GFP2 plasmid where it should be. In well 13 is the red box around the band for confirmation of pFMDV1/NLS. Wells 14 through 17 results were either contaminated or inconclusive.

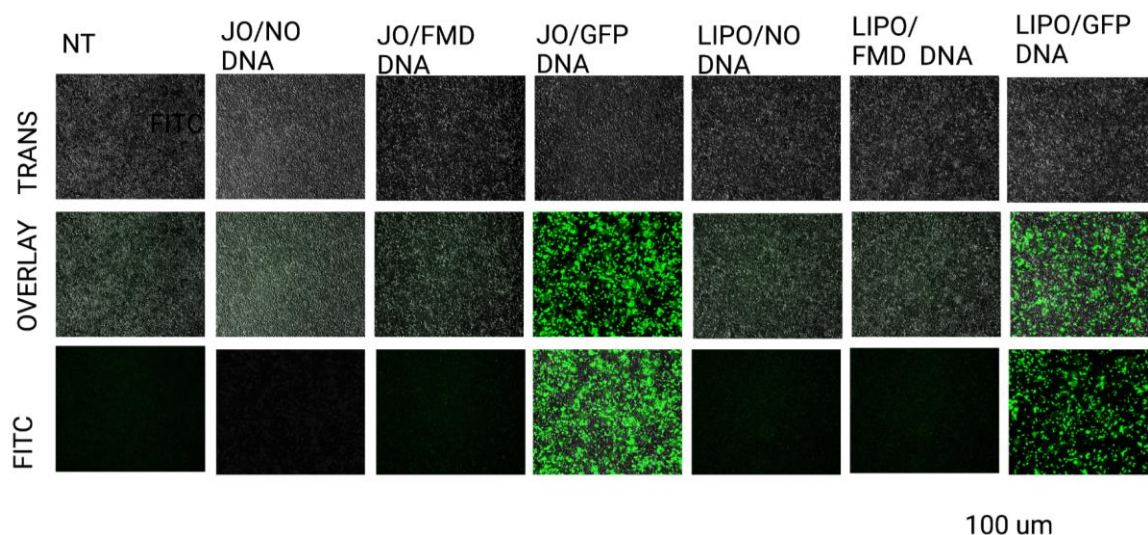


Figure 3.10. Images taken 24 hours after transfection with the Revolve Echo RF Upright Inverted Brightfield and Fluorescence Hybrid Microscope with 1.0 Zoom and 4X objective lens using the FITC channel for GFP and TRANS channel for normal features including overlay settings were used for immunofluorescence microscopy of transfected CHO cells, GFP plasmid, and FMD plasmid respectively.

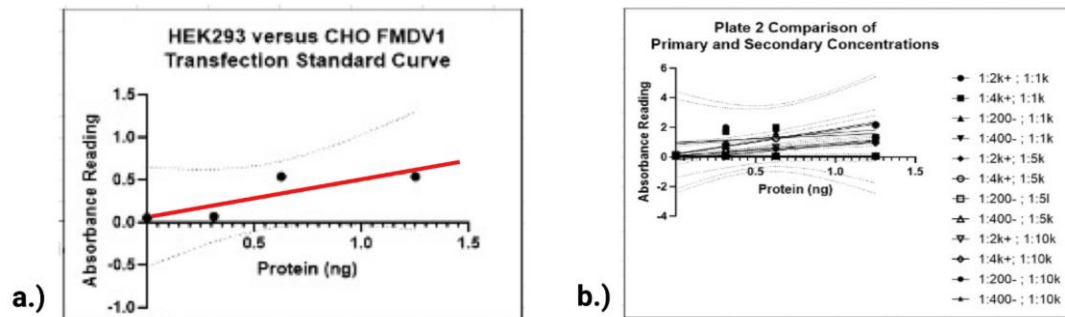


Figure 3.11. Simple linear regression for two individual troubleshooting plates to determine standard control for testing protein lysates. On the left (a.) is the final standard curve used for testing lysates as seen by the red line. On the right is process of testing dilution factors for determining which concentrations to use for standard curve.

Graphs in Figure 3.11 showing final standard curve and comparison of possible combinations of antibody concentrations testing for a difference in slopes using GraphPad Prism 8 (GraphPad Software). In Figure 3.11.b. there was no significant difference in slopes and intercepts. All the positive primaries paired with the 1:1000 secondaries were not significant either. Because 1:4000 primary and 1:10k secondary was significant and uses less reagent than other significant values even though 1:2000 and 1:10k has higher concentration. value for plate one for slope comparison .5912. For plate 2, p value is 0.0855. Results from Figure 3.11.b indicated the only significant values included 1:2000 and 1:5000 secondary that had a p value of 0.0205. The final standard curve used was a 1:4000 working dilution for both primary antibodies and 1:10,000 working dilution for secondary antibody concentrations.

Lysate results using Plate layout as seen in Figure 3.11.a. showed no significance with any values that did show detectable amounts of protein concentration in groups where there shouldn't of shown detection including non-transfected groups for both CHO and HEK, and also signs of protein expression for groups with just lipofectamine in HEK 293 and just JetOptimus in CHO-K1 cells. There was also no significant correlation between cell lines and because of controls testing positive for protein expression, no inference can be made on whether either cell line is superior to the other.

3.3. Discussion

FMDV is a ss (+) RNA *Aphthovirus* responsible for the cloven hooved disease, FMD. Domesticated cattle are especially susceptible and wild African buffalo act as a maintenance host shedding aerosolized virus particles for 3 to 5 years. FMD is rampant in lower economic areas such as parts of Asia, India and Africa. Symptoms of FMD include lesions, lameness, decreased milk production, and deaths in calves associated with myocarditis. Current treatment methods include an emergency live attenuated vaccine available upon approval from the OIE. Alternative treatment options especially in endemic regions must rely on quarantining, culling, and vaccinating the non-infected. In addition, these vaccines require a cold chain to maintain viability and a considerably short shelf life. Other disadvantages faced with current vaccination methods include only stimulating humoral immune responses and thus failing to provide long term protection against intracellular viruses. Additionally, no vaccine currently available offers protection outside of a specific strain. DNA vaccination offers the potential to offer cross-protection as well as stimulating both a humoral immune response and invoking a cell-mediated response. DNA is a naturally stable molecule that offers more predictable outcomes, increased shelf life, and can be stored at room temperature. DNA vaccines also have the added advantage of rapid manufacturing at a much lower cost overall.

The specific approach discussed in this paper consists of a DNA vaccine encoding the VP1 empty capsid that would eliminate the risk many other vaccines face such as toxicity, risk of viral transmission or thermal degradation. The VP1 polyprotein used in this thesis is from Serotype O that was geared towards cross protection against other strains within multiple topotypes as well. The immunodominant proteins selected from this polyprotein sequence

obtained through NCBI and aligned then blasted with other FMDV serotype O strains available to find conserved regions for optimal epitope selection. Primers were then designed specifically for the pFMDV1 isolate protein DNA sequence using NCBI Primer Blast and IDT. These primers were then used to amplify the FMDV1 DNA sequence through Polymerase Chain Reaction. The sequences were then checked for proper size using gel electrophoresis then sent to Gene Laboratory for proper sequence verification. Once DNA products were verified the amino acid sequence of the FMDV product was analyzed through IEDB for epitope selection. Immunogenetic epitopes with an immunogenicity score of 5 % or lower (high chance of electing an immune response) were selected for incorporation into an already finished backbone vector used for vaccine design. The full vaccine design included regions of the immunogenic epitope with FRS used as spaces in-between each one to mimic natural folding and turning, a SV40 NLS sequence was added to the end of the epitope sequence. Codon Optimization using IDT was performed to *bos taurus* and the DNA sequence generated was ordered through IDT and called FMD1. Once received, the FMD1 construct was transfected into chemically competent *E. coli* cells to amplify the DNA product. A CMV promoter was added through digestion of both the vaccine and promoter counterparts then ligated into the pBS backbone vector. This DNA was transfected into competent *E. coli* and amplified through PCR then checked for proper size using gel electrophoresis. Once that sequence was verified by the Gene Laboratory, a Maxikit was performed on the cells then harvested for cell culture. A control for ELISA detection of FMD vaccine was then optimized for all future FMD DNA antibody detection. The DNA sequence was transfected into CHO and HEK cells. ELISA test was performed on serum to determine if any detectable amount of protein expression occurred. The initial project design focused on a disease for which we were under the assumption we would have access to the antigens provided

from a researcher from Plumb Island where the only available vaccine antigen concentrates were stored. Had we known this specific Plumb Island researcher would not follow through, we would have chosen a different disease. Unfortunately, as a result we were unable to procure the antigens for this disease and used a specific component of the actual backbone vector for the vaccine to use as a primary protein for establishing standard curve of the ELIS. No statistically significant data was determined using the ELISA on detectable protein expression therefore no definitive statement can be made on if one transfection reagent outperformed the other as well if there was an optimal cell line. RT-PCR did confirm transcription in all transfection groups for CHO-K1 cell line with no detectable transcription activity in HEK-293. Theoretically, if adequate protein expression was detected after repeating the cell culture enough time for statistically significant data, then the vaccine would be tested in a possible quail model via in vivo testing for humoral and cellular-mediated immune response.

Possible adjustments to consider for better protein expression would be to conduct a second cell culture experiment using pCPP instead of removing it, therefore utilizing the selection marker that is suitable for eukaryotic cell culture testing. Specific changes that can be made for future experimentation include changing the amount of FBS added to total serum content. If there was a significant difference in the amount of protein secreted this would warrant proceeding into *in-vivo* testing where a pilot animal trial would take place. *In-vitro* transfection reagents can differ greatly from their effect on transfection and gene transfer in a controlled microenvironment versus how it would react through systematic administration with *in vivo*. Dr. Richard Cooper is currently in the process of designing a potential vehicular model to transport the vaccine using advanced technology such as 3D printing.

3.3. Conclusion

With further research and sufficient resources, the use of this vaccine design could demonstrate protective potential and contribute to helping create an alternative solution to the endemic raiding livestock and the livelihoods of individuals affected by this devastating virus. The public sphere is constantly pressing for new and innovative solutions to combat the omnipresent threat of emerging infectious diseases world-wide, but these advances are only beneficial for those who can afford it. This fails to create a solution that reaches those in less developed countries. There needs to be more committed action towards creating solutions for those who cannot access the scientific tools or available vaccinations. Even the most conscientious proposals or plan of action lacks alternative methodology for those who do not have access to the necessary resources and technology available. Current vaccines and treatments offered to those at war with FMDV are not grounded in existing local practices. Eradication is essentially only available in realms with advanced technology and developed economies. In these countries, any new threat from emerging pathogens is met with efficient and effective elimination to achieve a disease-free status. Access to vaccines, disease surveillance, and infectious disease public health infrastructure offer an impressive arsenal against pathogenic threat. For less developed countries, access to these amenities is no more than an abstract idea. The significance of this research is advancing the optimization of potential DNA vaccine designs that can help pave the way towards an economically viable solution for the prevention and control of emerging infectious disease where it is most desperately needed.

Appendix A: Experimental Data and Protocols

A.1. Experimental Data

Protein Outputs comparing HEK vs. CHO cell line:

Cell Sample	Primary Treatment	Interpolated Protein Amount	Data Entered	
H FMD+L	+	0.0123224977481619	0.057	
H FMD+L	-	0.0134595763305291	0.0575	
HFMD+JO	+		0.0465	
HFMD+JO	-	0.0327899122307701	0.066	
HLIPO	+		0.0465	
HLIPO	-		0.0435	
HJO	+		0.0485	
HJO	-		0.048	
HNT	+	0.000951711924490728	0.052	
HNT	-	0.0123224977481619	0.057	
CNT	+	0.04074946230734	0.0695	
CNT	-	0.0168708120776304	0.059	
CJO	+		0.0505	
CJO	-		0.048	
CLIPO	+		0.048	
CLIPO	-	0.050983169548644	0.074	
CFMDL	+	0.0589427196252139	0.0775	
CFMDL	-	0.0896438413491261	0.091	
CFMDJO	+	0.0771359769430879	0.0855	
CFMDJO	-	0.151046084796951	0.118	

A.2 Protocols:

Transformation Protocol

1. DNA of FMD1 Vector was delivered and eluted with 20 ul of DNA Elution Buffer added directly to tube. Dam negative competent cells found in -80 freezer.
2. 1 ul of DNA dilution were then added immediately to 50 ul of dam – competent cells.
3. Place mix on ice for 30 minutes

4. Heat shock at 42 C for 30 seconds
5. Place mix on ice for 5 minutes
6. Pipette 950 ul of room temp SOC media into mixture
7. Place in incubator at 37 C ° for 60 minutes.
8. Warm 2 selection agar plates (½ SB AMP) for growing colonies.
9. 100 ul of transformation mix on each plate was spread evenly on plates and left in 37 C Incubator for 24 hours.
10. Each colony will be swabbed with a sterile toothpick then swirled in 1 ml of ½ SB AMP Broth and placed in shaking incubator overnight at 37 C °
11. After every miniprep, midiprep, or maxiprep a freezback of stock culture broth in aliquotes of 1 ml each will be stored in -80 freezer.

Digestion Protocol:

1. Prepare mixture in PCR tube starting with 5 ul of DNA (from miniprep or other Zymopure prep kit)
2. DNA followed by 5 ul of 10x Fast Green Buffer
3. 1 ul of each enzyme desired for digestion
4. 38 ul of dH2O was pipetted last and mixed by centrifuging for 3 seconds to ensure homogeneity.
5. PCR mix was incubated at 37 C ° for 4 hours then heat shocked for 10 minutes at 65F

Gel Electrophoresis Protocol:

1. Select desired casting tray and numbered well comb in correct position. Measure TAE Buffer needed in graduated cylinder before pouring in glass flask.
 - 1.1 For a small gel, measure out 50 ml of TAE buffer.

- 1.2 For a large gel measure out 100 ml of TAE buffer.
- 1.3 For a SyberSafe gel, measure out premade SyberSafe solution (made in-house) instead of TAE buffer but the amount required depending on size of gel stays the same.
2. Ethidium bromide is then pipetted directly out of Amresco stock bottle directly into flask
 - 2.1 For a small gel, measure out 2.5 ul of EB.
 - 2.2 For a large gel, measure out 5 ul of EB.
 - 2.3 For a SyberSafe, NO ethidium bromide is added.
3. Microwave 1-3 minutes then cool down by gently swirling flask while in chorus running bottom of flask under dH₂O.
4. Pour into tray and wait for solidification.
 - 4.1 SyberSafe requires a cover or box for remaining duration of protocol due to light sensitivity
5. Once solidified, remove comb, and prepare wells by pipetting desired amount. Place tray into the BIORAD Power Pac 300 and ensure gel is fully submerged in fresh 1 X TAE Buffer (made in-house) with negative node (black) at starting position of wells to ensure samples move toward opposite end where the positive node (red) will be.
6. Parameters for BIORAD Power Pac 300 are set at constant 'A', mA at 60 followed by allotted time.

Ligation Protocol for Cloning with Instant Sticky-end Ligase Master Mix (M0370):

1. Transfer master mix to ice prior to set up. Mix tube by vortex for one second.
2. Combine desired ul of vector and ul DNA(3-fold molar excess) of insert and adjust volume to 5ul with dH₂O.

3. Add 5 ul of Instant Sticky-end Ligase Master Mix thoroughly by pipetting up and down 7-10 times, and place on ice. No heat inactivation is necessary. The sample is now ready to be used for transformation.

****Heat activation dramatically reduces transformation efficiency.**

****In-house treating has demonstrated that maximal transformation efficiency is achieved using between 20-100 ng of vector (sticky) and a corresponding 3-fold molar excess of the insert to be ligated into the vector.**

10X PBS Protocol:

For the final concentration, 160 grams of Sodium Chloride (NaCl, 140 mM), 4 grams of Potassium dihydrogen phosphate (KH_2PO_4 , 1.5 mM), 43.4 grams of sodium phosphate dibasic heptahydrate ($\text{Na}_2\text{HPO}_4 \cdot 7\text{H}_2\text{O}$, 8.0 mM), 4 grams of Potassium Chloride (KCl, 2.7 mM), and was diluted in 2.3 liters of Laboratory distilled water (DW) purified using a Millipore Synergy UV filtration and purification system (Synergy, Cat. # F1HB91145). The 10X PBS was homogenized using a magnetic stirrer on a magnetic warmer plate for one hour. The solution was then autoclaved as an extra precautionary step for ensuring all salts were fully dissolved and sterile before use. The stock solution of 10X Phosphate Buffered Saline (PBS) alone is not the correct pH for this specific wash buffer solution. By diluting the freshly made 10X PBS stock solution with 0.5% of Tween 20 (0.5%, v/v, Amresco Cat.#1894B76) and DW, the formulation will be at a desired pH of 7.4 and necessary for cells to maintain stability and survive in their microenvironment.

1% BSA

1% Bovine Serum Albumin (BSA)(Angio-Proteomie, Cat.# CAP-46) in 10X PBS /20% Tween-20 used as a blocking buffer by repelling nonspecific binding sites and used again to dilute antibodies for assays. Carbonate buffer solution, 9.6 pH, for coating plates were formulated so pH should not have to be adjusted.

ELISA Protocol:

Purpose: Prepare ELISA plates for testing protein under previously used conditions.

Day 1:

1. Protein Dilutions were put on a plate (100 ul per well). Carbonate Buffer made by Mack was added to the plates, 100 ul/ well.
2. Plates were covered and placed on the shaker incubator for 2 min. Then, they were moved to the 4 C for storage / incubation overnight.

Day 2:

1. Plate warmed to room temp for 30 mins.
2. Plates dumped and blocked with a fresh made blocking buffer with 200 ul/ well. Sticker placed on.

BSA 1% Mix: 4%:

§ 1 g BSA.	4 grams
§ 250 ul 20% Tween 20	1 ml
§ 100 ml 10 x PBS.	400 mLs

3. 2 hour incubation on shaker incubator. Make primary and secondary dilutions and leave out primary while putting secondary in the fridge).
4. “Bleach plate” ran through the washer with a bleach solution before doing the wash step.

5. The coated plate on shaker was dumped and tapped dry and plate was washed with freshly made PBS WASH buffer with settings on P08/M08

WASH Buffer Protocol:

2.5 ml 20% Tween 20

100 ml 10x DPBP

dH2O to 1 L

6. Plate was tapped dry and loaded with 100 ul/well of primary. Sticker placed back on.
7. 2-hour incubation on shaker incubation (Take out secondary out of fridge)
8. Plate dumped and tapped dry then was washed with PBS WASH buffer.
9. Plate tapped dry and coated with 100 ul of Secondary Protein (@ room temp). Sticker placed back on.
10. 2-hour incubation on shaker incubator.
11. Plate was dumped and tapped dry then washed with PBS WASH buffer.
12. Plate was tapped dry 100 ul/well TMB (room temp) loaded in the **DARK**
13. Incubated on plate shaker for 15-30 minutes depending on development
14. Stopped development with 2M sulfuric acid – 100ul/well.

References

1. Kamer, G., Nicklin, M. J., & Wimmer, E. (1984). Similarity in gene organization and homology between proteins of animal picomaviruses and a plant comovirus suggest common ancestry of these virus families. *Nucleic Acids Research*, 12(18), 7251–7267.
<https://doi.org/10.1093/nar/12.18.7251>
2. Baxt, B. (2004, April). Foot-and-Mouth Disease. *Clinical Microbiology Reviews*, 17(2), 465–493. <https://doi.org/10.1128/cmr.17.2.465-493.2004>
3. Maclachlan, B. V. S. M. S., N. James Maclachlan, B. V. S. M. S., & Dubovi, E. J. (2017). Fenner's Veterinary Virology. In *Chapter 26 : Pocornaviridae* (Fifth Edition, pp. 477–495). Elsevier Gezondheidszorg.
4. Jamal, S. M., & Belsham, G. J. (2013). Foot-and-mouth disease: past, present and future. *Veterinary Research*, 44(1), 116. <https://doi.org/10.1186/1297-9716-44-116>
5. Shang, J., & Sun, Y. (2021). CHEER: Hierarchical taxonomic classification for viral metagenomic data via deep learning. *Methods*, 189, 95–103.
<https://doi.org/10.1016/j.ymeth.2020.05.018>
6. Koonin, E. V., Krupovic, M., & Agol, V. I. (2021, August 18). The Baltimore Classification of Viruses 50 Years Later: How Does It Stand in the Light of Virus Evolution? *Microbiology and Molecular Biology Reviews*, 85(3). <https://doi.org/10.1128/mmbr.00053-21>
7. Walker, P. J., Siddell, S. G., Lefkowitz, E. J., Mushegian, A. R., Adriaenssens, E. M., Dempsey, D. M., Dutilh, B. E., Harrach, B., Harrison, R. L., Hendrickson, R. C., Junglen, S., Knowles, N. J., Kropinski, A. M., Krupovic, M., Kuhn, J. H., Nibert, M., Orton, R. J., Rubino, L., Sabanadzovic, S., . . . Davison, A. J. (2020). Changes to virus taxonomy and the Statutes ratified by the International Committee on Taxonomy of Viruses (2020). *Archives of Virology*, 165(11), 2737–2748. <https://doi.org/10.1007/s00705-020-04752-x>
8. Kuhn, J. H. (2021). Virus Taxonomy. *Encyclopedia of Virology*, 28–37.
<https://doi.org/10.1016/b978-0-12-809633-8.21231-4>
9. Rowlands, D. (2008a). Foot and Mouth Disease Viruses. *Encyclopedia of Virology*, 265–274. <https://doi.org/10.1016/b978-012374410-4.00402-7>
10. King, A. M. Q., F. Brown, P. Christian, T. Hovi, T. Hyypia, N. J. Knowles, S. M. Lemon, P. D. Minor, A. C. Palmenberg, T. Skern, and G. Stanway. 2000. Picornaviridae, p. 657-673. In M. H. V. van Regenmortel, C. M. Fauquet, D. H. L. Bishop, E. B. Carstens, M. K. Estes, S. M. Lemon, J. Maniloff, M. A. Mayo, D. J. McGeoch, C. R. Pringle, and R. B. Wickner. (ed.), *Virus taxonomy: classification and nomenclature of viruses. Seventh report of the International Committee on Taxonomy of Viruses*. Academic Press, San Diego, Calif.

11. Butler, J. M. (2015). Troubleshooting Data Collection. *Advanced Topics in Forensic DNA Typing: Interpretation*, 183–210. <https://doi.org/10.1016/b978-0-12-405213-0.00008-7>
12. Rodríguez-Habibe, I., Celis-Giraldo, C., Patarroyo, M. E., Avendaño, C., & Patarroyo, M. A. (2020). A Comprehensive Review of the Immunological Response against Foot-and-Mouth Disease Virus Infection and Its Evasion Mechanisms. *Vaccines*, 8(4), 764. <https://doi.org/10.3390/vaccines8040764>
13. Brito, B., Pauszek, S. J., Hartwig, E. J., Smoliga, G. R., Vu, L. T., Dong, P. V., Stenfeldt, C., Rodriguez, L. L., King, D. P., Knowles, N. J., Bachanek-Bankowska, K., Long, N. T., Dung, D. H., & Arzt, J. (2018). A traditional evolutionary history of foot-and-mouth disease viruses in Southeast Asia challenged by analyses of non-structural protein coding sequences. *Scientific Reports*, 8(1). <https://doi.org/10.1038/s41598-018-24870-6>
14. Knowles, N., Di Nardo, A., Wadsworth, J., King, D., & Bachanek-Bankowska, K. (2019). A47 Reconstructing the evolutionary history of pandemic foot-and-mouth disease viruses: The impact of recombination within the emerging O/ME-SA/Ind-2001 lineage. *Virus Evolution*, 5(Supplement_1). <https://doi.org/10.1093/ve/vez002.046>
15. ALI, W., HABIB, M., & SALAH UD DIN SHAH, M. (2018). Evaluation of PCR primers targeting the VP2 region of the foot-and-mouth disease virus for improved serotype detection. *TURKISH JOURNAL OF VETERINARY AND ANIMAL SCIENCES*, 42(4), 335–345. <https://doi.org/10.3906/vet-1801-17>
16. Brooksby, J.B., & Rogers, J. (1957). Methods used in typing the virus of foot-and-mouth disease at Pirbright, 1950–55. In, *Methods of typing and cultivation of foot-and-mouth disease virus: Project No. 208* (31-34). Paris, France: European Productivity Agency of the Organisation for European Economic Co-operation (OEEC).
17. Vallée, H., & Carré, H. (1922). Sur la pluralité du virus aphteux. *Comptes rendus de l'Académie des sciences Paris*, 174, 1498-1500.
18. Waldmann, O., & Trautwein, K. (1926). Experimentelle Untersuchungen über die Pluralität des Maul-und Klauenseuchevirus. *Berliner tierärztliche Wochenschrift*, 42, 569–571.
19. Brooksby, J. B. (1958). The virus of foot-and-mouth disease. *Advances in Virus Research*, 5, 1-37.
20. Dhanda, M.R., Gopalakrishnan, V.R., Dhillon, H.S. (1957). Note on the occurrence of atypical strains of foot-and-mouth diseases virus in India. *Indian Journal of Veterinary Science and Animal Husbandry*, 27, 79–84.
21. Samuel, A. R., & Knowles, N. J. (2001). Foot-and-mouth disease type O viruses exhibit genetically and geographically distinct evolutionary lineages (topotypes). *Journal of General Virology*, 82(3), 609–621. <https://doi.org/10.1099/0022-1317-82-3-609>

22. Foot-and-Mouth Disease Virus Serotypes, Topotypes and Lineages | Reference Laboratory for Foot-and-Mouth Disease. (n.d.). <https://www.foot-and-mouth.org/FMDV-nomenclature-working-group/nomenclature>
23. Gao, Y., Sun, S. Q., & Guo, H. C. (2016). Biological function of Foot-and-mouth disease virus non-structural proteins and non-coding elements. *Virology Journal*, 13(1). <https://doi.org/10.1186/s12985-016-0561-z>
24. Wang, D., Fang, L., Li, P., Sun, L., Fan, J., Zhang, Q., Luo, R., Liu, X., Li, K., Chen, H., Chen, Z., & Xiao, S. (2011). The Leader Proteinase of Foot-and-Mouth Disease Virus Negatively Regulates the Type I Interferon Pathway by Acting as a Viral Deubiquitinase. *Journal of Virology*, 85(8), 3758–3766. <https://doi.org/10.1128/jvi.02589-10>
25. Ward, JC, Snowden, JS, Herod, MR, Rowlands, DJ, Stonehouse, NJ. Functional advantages of triplication of the 3B coding region of the FMDV genome. *The FASEB Journal*. 2021; 35:e21215. <https://doi.org/10.1096/fj.202001473RR>
26. Zhu, Z., Yang, F., Cao, W., Liu, H., Zhang, K., Tian, H., Dang, W., He, J., Guo, J., Liu, X., & Zheng, H. (2019). The Pseudoknot Region of the 5' Untranslated Region Is a Determinant of Viral Tropism and Virulence of Foot-and-Mouth Disease Virus. *Journal of Virology*, 93(8). <https://doi.org/10.1128/jvi.02039-18>
27. Ward, J. C., Lasecka-Dykes, L., Neil, C., Adeyemi, O. O., Gold, S., McLean-Pell, N., Wright, C., Herod, M. R., Kealy, D., Warner, E., Jackson, T., King, D. P., Tuthill, T. J., Rowlands, D. J., & Stonehouse, N. J. (2022). The RNA pseudoknots in foot-and-mouth disease virus are dispensable for genome replication, but essential for the production of infectious virus. *PLOS Pathogens*, 18(6), e1010589. <https://doi.org/10.1371/journal.ppat.1010589>
28. Tycowski, K. T., Guo, Y. E., Lee, N., Moss, W. N., Vallery, T. K., Xie, M., & Steitz, J. A. (2015). Viral noncoding RNAs: more surprises. *Genes & Development*, 29(6), 567–584. <https://doi.org/10.1101/gad.259077.115>
29. Li, K., Wang, C., Yang, F., Cao, W., Zhu, Z., & Zheng, H. (2021). Virus–Host Interactions in Foot-and-Mouth Disease Virus Infection. *Frontiers in Immunology*, 12. <https://doi.org/10.3389/fimmu.2021.571509>
30. Zhu, J. J., Arzt, J., Puckette, M. C., Smoliga, G. R., Pacheco, J. M., & Rodriguez, L. L. (2013). Mechanisms of Foot-and-Mouth Disease Virus Tropism Inferred from Differential Tissue Gene Expression. *PLoS ONE*, 8(5), e64119. <https://doi.org/10.1371/journal.pone.0064119>
31. Wang, G., Wang, Y., Shang, Y., Zhang, Z., & Liu, X. (2015). How foot-and-mouth disease virus receptor mediates foot-and-mouth disease virus infection. *Virology Journal*, 12(1). <https://doi.org/10.1186/s12985-015-0246-z>

32. Monaghan P, Gold S, Simpson J, Zhang Z, Weinreb PH, Violette SM, et al. The alpha(v)beta6 integrin receptor for Foot-and-mouth disease virus is expressed constitutively on the epithelial cells targeted in cattle. *J Gen Virol*. 2005;86:2769–80.
33. Jackson T, Sheppard D, Denyer M, Blakemore W, King AM. The epithelial integrin alphavbeta6 is a receptor for foot-and-mouth disease virus. *J Virol*. 2000;74:4949–56.
34. Jackson T, Mould AP, Sheppard D, King AM. Integrin alphavbeta1 is a receptor for foot-and-mouth disease virus. *J Virol*. 2002;76:935–41.
35. Brown JK, McAleese SM, Thornton EM, Pate JA, Schock A, Macrae AI, et al. Integrin-alphavbeta6, a putative receptor for foot -and -mouth disease virus, is constitutively expressed in ruminant airways. *J Histochem Cytochem*. 2006;54:807–16.
36. Ruiz-Sáenz J, Goez Y, Tabares W, López-Herrera A. Cellular receptors for foot and mouth disease virus. *Intervirology*. 2009;52:201–12.
37. O'Donnell V, Larocco M, Baxt B. Heparan sulfate-binding foot-and-mouth disease virus enters cells via caveola-mediated endocytosis. *J Virol*. 2008;82:9075–85.
38. Moffat, K., Howell, G., Knox, C., Belsham, G. J., Monaghan, P., Ryan, M. D., & Wileman, T. (2005). Effects of Foot-and-Mouth Disease Virus Nonstructural Proteins on the Structure and Function of the Early Secretory Pathway: 2BC but Not 3A Blocks Endoplasmic Reticulum-to-Golgi Transport. *Journal of Virology*, 79(7), 4382–4395. <https://doi.org/10.1128/jvi.79.7.4382-4395.2005>
39. Rust, R. C., Ochs, K., Meyer, K., Beck, E., & Niepmann, M. (1999). Interaction of Eukaryotic Initiation Factor eIF4B with the Internal Ribosome Entry Site of Foot-and-Mouth Disease Virus Is Independent of the Polypyrimidine Tract-Binding Protein. *Journal of Virology*, 73(7), 6111–6113. <https://doi.org/10.1128/jvi.73.7.6111-6113.1999>
40. Puckette, M., Clark, B. A., Smith, J. D., Turecek, T., Martel, E., Gabbert, L., Pisano, M., Hurtle, W., Pacheco, J. M., Barrera, J., Neilan, J. G., & Rasmussen, M. (2017). Foot-and-Mouth Disease (FMD) Virus 3C Protease Mutant L127P: Implications for FMD Vaccine Development. *Journal of Virology*, 91(22). <https://doi.org/10.1128/jvi.00924-17>
41. Cheney, I. W., Naim, S., Shim, J. H., Reinhardt, M., Pai, B., Wu, J. Z., Hong, Z., & Zhong, W. (2003). Viability of Poliovirus/Rhinovirus VPg Chimeric Viruses and Identification of an Amino Acid Residue in the VPg Gene Critical for Viral RNA Replication. *Journal of Virology*, 77(13), 7434–7443. <https://doi.org/10.1128/jvi.77.13.7434-7443.2003>
42. Colenutt, C., Brown, E., Nelson, N., Paton, D. J., Eblé, P., Dekker, A., Gonzales, J. L., & Gubbins, S. (2020). Quantifying the Transmission of Foot-and-Mouth Disease Virus in Cattle via a Contaminated Environment. *MBio*, 11(4). <https://doi.org/10.1128/mbio.00381-20>

43. Baron, S., & Fleischmann Jr., W. R. (1996). *Viral Genetics* (4th edition). University of Texas Medical Branch at Galveston.
44. Ranjan, R., Biswal, J. K., Subramaniam, S., Singh, K. P., Stenfeldt, C., Rodriguez, L. L., Pattnaik, B., & Arzt, J. (2016). Foot-and-Mouth Disease Virus-Associated Abortion and Vertical Transmission following Acute Infection in Cattle under Natural Conditions. *PLOS ONE*, 11(12), e0167163. <https://doi.org/10.1371/journal.pone.0167163>
45. HOLLEY, C. (2017). Controlling swine diseases in Asia through the FAO/OIE Global Framework for the Progressive Control of Transboundary Animal Diseases (GF-TADs). *Bulletin De L'OIE*, 2017(3), 61–64. <https://doi.org/10.20506/bull.2017.3.2701>
46. *World Reference Laboratory for Foot-and-Mouth Disease*. (n.d.). Retrieved November 3, 2022, from <https://www.wrlfmd.org/about-us>
47. OIE/Food and Agriculture Organization (FAO) Foot-and-Mouth Disease Reference Laboratory Network. (2018). *Annual Report*. <https://www.foot-and-mouth.org/sites/foot/files/user-files/research-paper/pdf/11-19/OIE-FAO%20FMD%20Ref%20Lab%20Network%20Report%202018.pdf>
48. Abbas, L. K. A. A. H. (2022). *Basic Immunology: Functions and Disorders of the Immune System*, 6/SAE 2019 (6th ed.). Elsevier India.
49. Hollie-Donze, H. (2020). Recognizing Intruders [Class handout]. Louisiana State University, BIOL2051.
50. Medina, G. N., Segundo, F. D. S., Stenfeldt, C., Arzt, J., & de los Santos, T. (2018). The Different Tactics of Foot-and-Mouth Disease Virus to Evade Innate Immunity. *Frontiers in Microbiology*, 9. <https://doi.org/10.3389/fmicb.2018.02644>
51. Diaz-San Segundo, F., Moraes, M. P., de los Santos, T., Dias, C. C. A., & Grubman, M. J. (2010). Interferon-Induced Protection against Foot-and-Mouth Disease Virus Infection Correlates with Enhanced Tissue-Specific Innate Immune Cell Infiltration and Interferon-Stimulated Gene Expression. *Journal of Virology*, 84(4), 2063–2077. <https://doi.org/10.1128/jvi.01874-09>
52. BLANCO, P., PALUCKA, A., PASCUAL, V., & BANCHEREAU, J. (2008). Dendritic cells and cytokines in human inflammatory and autoimmune diseases. *Cytokine & Growth Factor Reviews*, 19(1), 41–52. <https://doi.org/10.1016/j.cytogfr.2007.10.004>
53. Borgoyakova, M. B., Karpenko, L. I., Rudometov, A. P., Shanshin, D. V., Isaeva, A. A., Nesmeyanova, V. S., Volkova, N. V., Belenkaya, S. V., Murashkin, D. E., Shcherbakov, D. N., Volosnikova, E. A., Starostina, E. V., Orlova, L. A., Danilchenko, N. V., Zaikovskaya, A. V., Pyankov, O. V., & Ilyichev, A. A. (2021). Immunogenic Properties of the DNA Construct Encoding the Receptor-Binding Domain of the SARS-CoV-2 Spike Protein. *Molecular Biology*, 55(6), 889–898. <https://doi.org/10.1134/s0026893321050046>

54. Lapinet, J. A., Scapini, P., Calzetti, F., Pérez, O., & Cassatella, M. A. (2000). Gene Expression and Production of Tumor Necrosis Factor Alpha, Interleukin-1 β (IL-1 β), IL-8, Macrophage Inflammatory Protein 1 α (MIP-1 α), MIP-1 β , and Gamma Interferon-Inducible Protein 10 by Human Neutrophils Stimulated with Group B Meningococcal Outer Membrane Vesicles. *Infection and Immunity*, 68(12), 6917–6923. <https://doi.org/10.1128/iai.68.12.6917-6923.2000>
55. Kim, H., Kim, A. Y., Choi, J., Park, S. Y., Park, S. H., Kim, J. S., Lee, S. I., Park, J. H., Park, C. K., & Ko, Y. J. (2021). Foot-and-Mouth Disease Virus Evades Innate Immune Response by 3C-Targeting of MDA5. *Cells*, 10(2), 271. <https://doi.org/10.3390/cells10020271>
56. Mahajan, S., Sharma, G. K., Bora, K., & Pattnaik, B. (2021). Identification of novel interactions between host and non-structural protein 2C of foot-and-mouth disease virus. *Journal of General Virology*, 102(3). <https://doi.org/10.1099/jgv.0.001577>
57. Deliyannis, G., Jackson, D. A., Dyer, W. B., Bates, J. E., Coulter, A., Harling-McNabb, L., & Brown, L. E. (1998). Immunopotential of humoral and cellular responses to inactivated influenza vaccines by two different adjuvants with potential for human use. *Vaccine*, 16(20), 2058–2068. [https://doi.org/10.1016/s0264-410x\(98\)00080-2](https://doi.org/10.1016/s0264-410x(98)00080-2)
58. Sumption, K., Rweyemamu, M., & Wint, W. (2008). Incidence and Distribution of Foot-and-Mouth Disease in Asia, Africa and South America; Combining Expert Opinion, Official Disease Information and Livestock Populations to Assist Risk Assessment. *Transboundary and Emerging Diseases*, 55(1), 5–13. <https://doi.org/10.1111/j.1865-1682.2007.01017.x>
59. About us / World Reference Laboratory for Foot-and-Mouth Disease. (n.d.). Retrieved November 3, 2022, from <https://www.wrlfmd.org/about-us>
60. DeLiberto, T., & Beach, R. H. (2006). USDA APHIS Wildlife Services' National Wildlife Disease Surveillance and Emergency Response System (SERS). *Proceedings of the Vertebrate Pest Conference*, 22. <https://doi.org/10.5070/v422110036>
61. Department for Environment, Food and Rural Affairs, Animal and Plant Health Agency. (n.d.). *Foot and Mouth Disease in South-East Asia* (VITT/1200 FMD in south-east Asia). Veterinary and Science Policy Advice Team - International Disease Monitoring.
62. Department for Environment, Food and Rural Affairs, Animal and Plant Health Agency. (n.d.). *Foot and Mouth Disease in South-East Asia* (VITT/1200 FMD in south-east Asia). Veterinary and Science Policy Advice Team - International Disease Monitoring.
63. Doel, T., & Pullen, L. (1990). International bank for foot-and-mouth disease vaccine: stability studies with virus concentrates and vaccines prepared from them. *Vaccine*, 8(5), 473–478. [https://doi.org/10.1016/0264-410x\(90\)90249-1](https://doi.org/10.1016/0264-410x(90)90249-1)
64. Häsler, B., Limon, G., Queenan, K., Rushton, J., Madege, M., Mlangwa, J., & Mghwira, J. (2021). Cost-benefit and feasibility analysis for establishing a foot-and-mouth disease free zone

in Rukwa region in Tanzania. *Preventive Veterinary Medicine*, 196, 105494.
<https://doi.org/10.1016/j.prevetmed.2021.105494>

65. Arzt, J., Juleff, N., Zhang, Z., & Rodriguez, L. L. (2011). The Pathogenesis of Foot-and-Mouth Disease I: Viral Pathways in Cattle. *Transboundary and Emerging Diseases*, 58(4), 291–304. <https://doi.org/10.1111/j.1865-1682.2011.01204.x>

66. Hardham, J. M. (2020a). Novel Foot-and-Mouth Disease Vaccine Platform: Formulations for Safe and DIVA-Compatible FMD Vaccines With Improved Potency. *Frontiers in Veterinary Science*, 7(554305). <https://doi.org/10.3389/fvets.2020.554305>

67. Bronsvoort, B., Toft, N., Bergmann, I. E., Sørensen, K. J., Anderson, J., Malirat, V., Tanya, V. N., & Morgan, K. L. (2006). Evaluation of three 3ABC ELISAs for foot-and-mouth disease non-structural antibodies using latent class analysis. *BMC Veterinary Research*, 2(1), 30. <https://doi.org/10.1186/1746-6148-2-30>

68. Berger, H. G., Straub, O., Ahl, R., Tesar, M., & Marquardt, O. (1990). Identification of foot-and-mouth disease virus replication in vaccinated cattle by antibodies to non-structural virus proteins. *Vaccine*, 8(3), 213–216. [https://doi.org/10.1016/0264-410x\(90\)90048-q](https://doi.org/10.1016/0264-410x(90)90048-q)

69. Bai, H., Lester, G. M., Petishnok, L., & Dean, D. (2017). Cytoplasmic transport and nuclear import of plasmid DNA. *Bioscience Reports*, 37(6). <https://doi.org/10.1042/bsr20160616>

70. Bidart, Z. M. (2020). Optimized Adenoviral Vector That Enhances the Assembly of FMDV O1 Virus-Like Particles in situ Increases Its Potential as Vaccine for Serotype O Viruses. *Frontiers Microbiology*. <https://doi.org/10.3389/fmicb.2020.591019>

71. García-Briones, M., Rosas, M. F., González-Magaldi, M., Martín-Acebes, M. A., Sobrino, F., & Armas-Portela, R. (2006). Differential distribution of non-structural proteins of foot-and-mouth disease virus in BHK-21 cells. *Virology*, 349(2), 409–421. <https://doi.org/10.1016/j.virol.2006.02.042>

72. Gubin, A., Koduru, S., Njoroge, J., Bhatnagar, R., & Miller, J. (1999). Stable Expression of Green Fluorescent Protein after Liposomal Transfection of K562 Cells without Selective Growth Conditions. *BioTechniques*, 27(6), 1162–1170. <https://doi.org/10.2144/99276st02>

73. Bai, H., Lester, G. M., Petishnok, L., & Dean, D. (2017). Cytoplasmic transport and nuclear import of plasmid DNA. *Bioscience Reports*, 37(6). <https://doi.org/10.1042/bsr20160616>

74. Schek, N., Cooke, C., & Alwine, J. C. (1992). Definition of the upstream efficiency element of the simian virus 40 late polyadenylation signal by using in vitro analyses. *Molecular and Cellular Biology*, 12(12), 5386–5393. <https://doi.org/10.1128/mcb.12.12.5386-5393.1992>

75. Dean, D. A., Dean, B. S., Muller, S., & Smith, L. C. (1999). Sequence Requirements for Plasmid Nuclear Import. *Experimental Cell Research*, 253(2), 713–722. <https://doi.org/10.1006/excr.1999.4716>

76. Lapinet, J. A., Scapini, P., Calzetti, F., Pérez, O., & Cassatella, M. A. (2000). Gene Expression and Production of Tumor Necrosis Factor Alpha, Interleukin-1 β (IL-1 β), IL-8, Macrophage Inflammatory Protein 1 α (MIP-1 α), MIP-1 β , and Gamma Interferon-Inducible Protein 10 by Human Neutrophils Stimulated with Group B Meningococcal Outer Membrane Vesicles. *Infection and Immunity*, 68(12), 6917–6923. <https://doi.org/10.1128/iai.68.12.6917-6923.2000>
77. Moulin, V., Morgan, M. E., Eleveld-Trancikova, D., Haanen, J. B. A. G., Wienders, E., Looman, M. W. G., Janssen, R. A. J., Figdor, C. G., Jansen, B. J. H., & Adema, G. J. (2012). Targeting dendritic cells with antigen via dendritic cell-associated promoters. *Cancer Gene Therapy*, 19(5), 303–311. <https://doi.org/10.1038/cgt.2012.2>
78. Rasmussen, L. K., Larsen, Y. B., & Højrup, P. (2005). Characterization of different cell culture media for expression of recombinant antibodies in mammalian cells: Presence of contaminating bovine antibodies. *Protein Expression and Purification*, 41(2), 373–377. <https://doi.org/10.1016/j.pep.2005.01.011>
79. Sudowe, S., Dominitzki, S., Montermann, E., Bros, M., Grabbe, S., & Reske-Kunz, A. B. (2009). Uptake and presentation of exogenous antigen and presentation of endogenously produced antigen by skin dendritic cells represent equivalent pathways for the priming of cellular immune responses following biolistic DNA immunization.
80. Suschak, J. J., Williams, J. A., & Schmaljohn, C. S. (2017). Advancements in DNA vaccine vectors, non-mechanical delivery methods, and molecular adjuvants to increase immunogenicity. *Human Vaccines & Immunotherapeutics*, 13(12), 2837–2848. <https://doi.org/10.1080/21645515.2017.1330236>
81. Mahajan, S., Sharma, G. K., Bora, K., & Pattnaik, B. (2021). Identification of novel interactions between host and non-structural protein 2C of foot-and-mouth disease virus. *Journal of General Virology*, 102(3). <https://doi.org/10.1099/jgv.0.001577>
82. Schek, N., Cooke, C., & Alwine, J. C. (1992). Definition of the upstream efficiency element of the simian virus 40 late polyadenylation signal by using in vitro analyses. *Molecular and Cellular Biology*, 12(12), 5386–5393. <https://doi.org/10.1128/mcb.12.12.5386-5393.1992>
83. <https://www.sciencedirect.com/science/article/abs/pii/S0882401018315080?via%3Dihub>
84. Altschul, S. F., Wootton, J. C., Gertz, E. M., Agarwala, R., Morgulis, A., Schaffer, A. A., & Yu, Y. K. (2005). Protein database searches using compositionally adjusted substitution matrices. *FEBS Journal*, 272(20), 5101–5109. <https://doi.org/10.1111/j.1742-4658.2005.04945.x>
85. Altschul, S. (1997). Gapped BLAST and PSI-BLAST: a new generation of protein database search programs. *Nucleic Acids Research*, 25(17), 3389–3402. <https://doi.org/10.1093/nar/25.17.3389>

86. Chong, Z. X., Yeap, S. K., & Ho, W. Y. (2021). Transfection types, methods and strategies: a technical review. *PeerJ*, 9, e11165. <https://doi.org/10.7717/peerj.11165>
87. de los Milagros Bassani Molinas, M., Beer, C., Hesse, F., Wirth, M., & Wagner, R. (2013). Optimizing the transient transfection process of HEK-293 suspension cells for protein production by nucleotide ratio monitoring. *Cytotechnology*, 66(3), 493–514. <https://doi.org/10.1007/s10616-013-9601-3>
88. Gubin, A., Koduru, S., Njoroge, J., Bhatnagar, R., & Miller, J. (1999). Stable Expression of Green Fluorescent Protein after Liposomal Transfection of K562 Cells without Selective Growth Conditions. *BioTechniques*, 27(6), 1162–1170. <https://doi.org/10.2144/99276st02>
89. Zhang, J., Shrivastava, S., Cleveland, R. O., & Rabbitts, T. H. (2019). Lipid-mRNA Nanoparticle Designed to Enhance Intracellular Delivery Mediated by Shock Waves. *ACS Applied Materials & Interfaces*, 11(11), 10481–10491. <https://doi.org/10.1021/acsami.8b21398>
90. Lee, C. H. (2009). Recombinant Green Fluorescent Protein Derivatives as a Fusion Tag for in vitro Experiments. *Interdisciplinary Bio Central*, 1(1), 1–15. <https://doi.org/10.4051/ibce.2009.1.0002>

Vita

Taylor Haynie, born in Baton Rouge, Louisiana and received her bachelor's degree in Animal Sciences from Louisiana State University (LSU). During her junior year, she studied abroad at the University of Sydney, NSW, Australia where she interned with a group of researchers in animal genetics. That is where her interest grew in genetics as well as working in a laboratory setting. She decided to enter the College of Agriculture at LSU to work under the supervision of Dr. Richard Cooper to complete her master's in Animal Science with a focus on Animal Genetics and Recombinant DNA Vaccination. Upon completion of her master's degree, she will begin looking for jobs as a research scientist in Houston, TX.